



OPEN ACCESS

EDITED BY

Rona A. R. McGill,
University of Glasgow, United Kingdom

REVIEWED BY

Vincent Balter,
Centre National de la Recherche
Scientifique (CNRS), France
Joshua Robinson,
Boston University, United States
Laszlo Kocsis,
Université de Lausanne, Switzerland

*CORRESPONDENCE

Tina Lüdecke
tina.luedecke@mpic.de
Jennifer N. Leichliter
jennifer.leichliter@mpic.de

†These authors have contributed
equally to this work and share first
authorship

‡These authors share senior authorship

SPECIALTY SECTION

This article was submitted to
Population, Community,
and Ecosystem Dynamics,
a section of the journal
Frontiers in Ecology and Evolution

RECEIVED 31 May 2022

ACCEPTED 27 October 2022

PUBLISHED 24 November 2022

CITATION

Lüdecke T, Leichliter JN, Aldeias V,
Bamford MK, Biro D, Braun DR,
Capelli C, Cybulski JD, Duprey NN,
Ferreira da Silva MJ, Foreman AD,
Habermann JM, Haug GH,
Martínez FI, Mathe J, Mulch A,
Sigman DM, Vonhof H, Bobe R,
Carvalho S and Martínez-García A
(2022) Carbon, nitrogen, and oxygen
stable isotopes in modern tooth
enamel: A case study from Gorongosa
National Park, central Mozambique.
Front. Ecol. Evol. 10:958032.
doi: 10.3389/fevo.2022.958032

Carbon, nitrogen, and oxygen stable isotopes in modern tooth enamel: A case study from Gorongosa National Park, central Mozambique

Tina Lüdecke^{1,2,3,4*†}, Jennifer N. Leichliter^{1,2,5*†}, Vera Aldeias⁶,
Marion K. Bamford⁷, Dora Biro^{8,9}, David R. Braun^{3,10,11},
Cristian Capelli^{8,12}, Jonathan D. Cybulski^{1,13,14},
Nicolas N. Duprey¹, Maria J. Ferreira da Silva^{15,16,17},
Alan D. Foreman¹, Jörg M. Habermann¹⁸, Gerald H. Haug^{3,19},
Felipe I. Martínez²⁰, Jacinto Mathe^{3,21}, Andreas Mulch^{4,22},
Daniel M. Sigman²³, Hubert Vonhof²⁴, René Bobe^{3,6,21},
Susana Carvalho^{3,6,21,25‡} and Alfredo Martínez-García^{1‡}

¹Organic Isotope Geochemistry Group, Max Planck Institute for Chemistry, Mainz, Germany, ²Emmy Noether Group for Hominin Meat Consumption, Max Planck Institute for Chemistry, Mainz, Germany, ³Primate Models for Behavioural Evolution, Institute of Human Sciences, University of Oxford, Oxford, United Kingdom, ⁴Senckenberg Biodiversity and Climate Research Centre, Frankfurt, Germany, ⁵Institute of Geosciences, Johannes Gutenberg University, Mainz, Germany, ⁶Interdisciplinary Center for Archaeology and Evolution of Human Behaviour, Universidade do Algarve, Faro, Portugal, ⁷Evolutionary Studies Institute, University of the Witwatersrand, Johannesburg, South Africa, ⁸Department of Zoology, University of Oxford, Oxford, United Kingdom, ⁹Department of Brain and Cognitive Sciences, University of Rochester, Rochester, NY, United States, ¹⁰Technological Primates Group, Max Planck Institute for Evolutionary Anthropology, Leipzig, Germany, ¹¹Center for the Advanced Study of Human Paleobiology, George Washington University, Washington, DC, United States, ¹²Department of Chemistry, Life Sciences and Environmental Sustainability, University of Parma, Parma, Italy, ¹³Smithsonian Tropical Research Institute, Balboa, Panama, ¹⁴Graduate School of Oceanography, University of Rhode Island, Narragansett, RI, United States, ¹⁵Centro de Investigação em Biodiversidade e Recursos Genéticos, InBIO Laboratório Associado, Universidade do Porto, Vairão, Portugal, ¹⁶BIOPOLIS Program in Genomics, Biodiversity and Land Planning, Centro de Investigação em Biodiversidade e Recursos Genéticos, Vairão, Portugal, ¹⁷Organisms and Environment Division, School of Biosciences, Cardiff University, Cardiff, United Kingdom, ¹⁸GeoZentrum Nordbayern, Friedrich-Alexander-Universität Erlangen-Nürnberg, Erlangen, Germany, ¹⁹Department of Climate Geochemistry, Max Planck Institute for Chemistry, Mainz, Germany, ²⁰Escuela de Antropología, Facultad de Ciencias Sociales, Pontificia Universidad Católica de Chile, Santiago, Chile, ²¹Gorongosa National Park, Sofala, Mozambique, ²²Institute of Geosciences, Goethe University Frankfurt, Frankfurt, Germany, ²³Department of Geosciences, Princeton University, Princeton, NJ, United States, ²⁴Inorganic Gas Isotope Geochemistry Group, Max Planck Institute for Chemistry, Mainz, Germany, ²⁵Centre for Functional Ecology, University of Coimbra, Coimbra, Portugal

The analyses of the stable isotope ratios of carbon ($\delta^{13}\text{C}$), nitrogen ($\delta^{15}\text{N}$), and oxygen ($\delta^{18}\text{O}$) in animal tissues are powerful tools for reconstructing the feeding behavior of individual animals and characterizing trophic interactions in food webs. Of these biomaterials, tooth enamel is the hardest, most mineralized vertebrate tissue and therefore least likely to be affected by chemical alteration (i.e., its isotopic composition can be preserved over millions of years), making it an important and widely available archive

for biologists and paleontologists. Here, we present the first combined measurements of $\delta^{13}\text{C}$, $\delta^{15}\text{N}$, and $\delta^{18}\text{O}$ in enamel from the teeth of modern fauna (herbivores, carnivores, and omnivores) from the well-studied ecosystem of Gorongosa National Park (GNP) in central Mozambique. We use two novel methods to produce high-precision stable isotope enamel data: (i) the “*oxidation-denitrification method*,” which permits the measurement of mineral-bound organic nitrogen in tooth enamel ($\delta^{15}\text{N}_{\text{enamel}}$), which until now, has not been possible due to enamel’s low organic content, and (ii) the “*cold trap method*,” which greatly reduces the sample size required for traditional measurements of inorganic $\delta^{13}\text{C}_{\text{enamel}}$ and $\delta^{18}\text{O}_{\text{enamel}}$ (from ≥ 0.5 to ≤ 0.1 mg), permitting analysis of small or valuable teeth and high-resolution serial sampling of enamel. The stable isotope results for GNP fauna reveal important ecological information about the trophic level, dietary niche, and resource consumption. $\delta^{15}\text{N}_{\text{enamel}}$ values clearly differentiate trophic level (i.e., carnivore $\delta^{15}\text{N}_{\text{enamel}}$ values are 4.0‰ higher, on average, than herbivores), $\delta^{13}\text{C}_{\text{enamel}}$ values distinguish C_3 and/or C_4 biomass consumption, and $\delta^{18}\text{O}_{\text{enamel}}$ values reflect local meteoric water ($\delta^{18}\text{O}_{\text{water}}$) in the park. Analysis of combined carbon, nitrogen, and oxygen stable isotope data permits geochemical separation of grazers, browsers, omnivores, and carnivores according to their isotopic niche, while mixed-feeding herbivores cannot be clearly distinguished from other dietary groups. These results confirm that combined C, N, and O isotope analyses of a single aliquot of tooth enamel can be used to reconstruct diet and trophic niches. Given its resistance to chemical alteration, the analysis of these three isotopes in tooth enamel has a high potential to open new avenues of research in (paleo)ecology and paleontology.

KEYWORDS

diet, ecology, trophic level reconstruction, food webs, vertebrate, savanna

Introduction

In modern ecosystems, stable isotope geochemistry can complement traditional ecological approaches (e.g., field observations and behavioral studies) and help researchers to better understand the dietary niche and habitat use of animals in the wild. The stable carbon ($\delta^{13}\text{C}$), nitrogen ($\delta^{15}\text{N}$), and oxygen ($\delta^{18}\text{O}$) isotope compositions of body tissues can provide information about an individual’s metabolism and feeding behavior, trophic interactions, and even record aspects of the (paleo)environment such as aridity, seasonality, and vegetation composition (e.g., DeNiro and Epstein, 1981; Ambrose, 1986; Cerling et al., 1997; Bocherens and Drucker, 2003; Kingston and Harrison, 2007; Segalen et al., 2007; Bocherens, 2009; Lüdecke et al., 2016, 2018).

In modern fauna, isotopic measurements are routinely conducted on a variety of biological materials such as collagen (from bone or dentin), soft tissues (e.g., muscle), and body fluids (e.g., blood and urea). Paleontologists have long sought

a reliably preserved tissue (i.e., without diagenetic alteration) in which to measure isotope ratios of all three elements—carbon, nitrogen, and oxygen—in deep time contexts. Tooth enamel, as the densest and most mineralized vertebrate tissue, has great potential in this respect (Leichliter et al., 2022). Hydroxyapatite content is about 95% wt. in mature enamel (Sakae et al., 1997; Passey and Cerling, 2002; Lacruz et al., 2017; Gil-Bona and Bidlack, 2020), which makes it more resistant to diagenetic alteration during fossilization than more porous and poorly mineralized tissues such as bone or dentin (mineralization ca. 70% wt.; Goldberg et al., 2011).

As such, the inorganic mineral phase of tooth enamel has long been the focus of carbon ($\delta^{13}\text{C}_{\text{enamel}}$) and oxygen ($\delta^{18}\text{O}_{\text{enamel}}$) stable isotope analyses for the reconstruction of the diet of extinct and extant species (Ambrose and Norr, 1993).

Typically, 500–1,000 μg of tooth enamel, which contains less than 5% structural carbonate, is needed for precise $\delta^{13}\text{C}_{\text{enamel}}$ and $\delta^{18}\text{O}_{\text{enamel}}$ analysis with traditional continuous-flow isotope ratio mass spectrometry. The “*cold trap method*” presented in

this study permits high-precision $\delta^{13}\text{C}_{\text{enamel}}$ and $\delta^{18}\text{O}_{\text{enamel}}$ analysis of as little as 50 μg tooth enamel. The method employs a cryofocusing step during which the sample gas is collected in a liquid N_2 trap (Vonhof et al., 2020a,b). This results in >80% reduction in the sample size typically required for conventional analyses (refer to e.g., Merceron et al., 2021; Jaouen et al., 2022).

Recently, Leichliter et al. (2021) showed that $\delta^{15}\text{N}_{\text{enamel}}$ records the nitrogen isotopic composition of an animal's diet under controlled conditions in a feeding experiment with rodents. The significant advantage of measuring $\delta^{15}\text{N}$ in tooth enamel ($\delta^{15}\text{N}_{\text{enamel}}$) instead of (bone/dentin) collagen is that enamel is more resistant to diagenesis (Lee-Thorp and Van der Merwe, 1987; Wang and Cerling, 1994; Koch et al., 1997; Koch, 2007). The dense mineralization of enamel thus has a high potential to protect inorganic components from isotopic alteration during fossilization (Leichliter et al., 2022). In fact, the tooth enamel biomineral matrix appears to act as a closed system during oxidative attack, dissolution, and thermal alteration, leaving the $\delta^{15}\text{N}_{\text{enamel}}$ value of a fossil unchanged (Martinez-Garcia et al., 2022), demonstrating the potential utility of $\delta^{15}\text{N}_{\text{enamel}}$ as a new trophic proxy in paleoecological studies. However, high-precision analysis of $\delta^{15}\text{N}_{\text{enamel}}$ in tooth enamel-bound nitrogen has been hampered by its low nitrogen content (about 0.5–2.5 g N/100 g in mature mammalian enamel; Teruel et al., 2015). To fill this gap in our isotopic toolbox, we recently developed a method to determine the nitrogen isotopic composition of the organic matter preserved in tooth enamel (Leichliter et al., 2021). This method, adapted from studies of marine microfossils (i.e., diatoms and foraminifera; Sigman et al., 2001; Robinson et al., 2004; Ren et al., 2009) and macrofossils (Wang et al., 2014, 2015, 2017; Lueders-Dumont et al., 2018; Kast et al., 2022), involves the oxidation of nitrogen in enamel-bound organic matter to nitrate, followed by bacterial conversion of nitrate to N_2O . This “oxidation-denitrification method” requires 5 nmol of N (i.e., 5 mg of enamel; Leichliter et al., 2021), which reflects ca. 1% of the material needed for conventional combustion measurements and ca. half the material used for nano-elemental analyzer measurements (e.g., Polissar et al., 2009; Fulton et al., 2018). Importantly, the “oxidation-denitrification method” drastically improves analytical precision from $\sim 1.0\%$ 1σ standard deviation for nano-EA measurements at 8 nmol of N (Fulton et al., 2018) to $<0.2\%$ at 5 nmol of N. This precision is more than sufficient to resolve the 3–5‰ trophic level enrichment in $\delta^{15}\text{N}$ observed in large-scale ecological studies (Schoeninger and DeNiro, 1984; Bocherens and Drucker, 2003; Caut et al., 2009).

Here, we present the first combined $\delta^{13}\text{C}_{\text{enamel}}$, $\delta^{15}\text{N}_{\text{enamel}}$, and $\delta^{18}\text{O}_{\text{enamel}}$ isotope data measured in the same aliquot of tooth enamel. We analyzed the tooth enamel of modern mammalian fauna (17 taxa; bovids, equids, suids, elephants, hippos, primates, felids) and one reptile (crocodiles) from Gorongosa National Park (GNP), a well-studied ecosystem in

central Mozambique (refer to e.g., Wilson, 2014; Correia et al., 2017; Atkins et al., 2019; Martinez et al., 2019; Pansu et al., 2019; Stalmans et al., 2019; Bobe et al., 2020; Guyton et al., 2020). In addition, we analyzed $\delta^{18}\text{O}_{\text{water}}$ of (permanent and ephemeral) lakes, ponds, streams, floodplains, rain-, and groundwater to evaluate isotope patterns of available drinking water, which are the main determinants of $\delta^{18}\text{O}_{\text{enamel}}$ in large mammals (Kohn and Cerling, 2002). With this dataset, we test two novel methods, as well as gain new insight into wild animal foraging behavior and the food web dynamics of GNP.

Tooth enamel as dietary proxy material

Dental material chronologically records the diet of an individual during a distinct time period in their life. During enamel maturation, the organic matrix is removed and replaced with inorganic minerals over a period of weeks, months, or years, depending on taxon, rate of wear, and tooth size (Ungar, 2010). Once mature enamel has fully mineralized, it has no regenerative capacity, and thus preserves an animal's isotopic composition during the time of tooth formation. This differentiates enamel from other tissues (e.g., soft tissues, but also bone or dentin) that undergo continuous remodeling (e.g., Balasse et al., 1999; Kohn and Cerling, 2002; Passey and Cerling, 2002; Zazzo et al., 2005; Abou Neel et al., 2016; Yang et al., 2020). Tooth enamel is, therefore, one of the only archives in the vertebrate body that records dietary information from early life stages (i.e., infant to young-adult) and that is also preserved in the fossil record. To reconstruct the adult diet and avoid the isotopic effect of breast milk consumption (Fuller et al., 2006; Tsutaya and Yoneda, 2015; Dailey-Chwalibóg et al., 2020; Chinique de Armas et al., 2022), we targeted the latest-forming permanent tooth (i.e., usually M3) in each specimen (for details refer to [Supplementary Data Sheet 1](#) and [Supplementary Table 1](#)).

For this study, we sampled bulk enamel, meaning that the resulting isotope data are time-averaged and record several months or even years depending on tooth mineralization rate (which can vary between taxa), as well as sampling strategy.

Isotope ratios for tooth enamel are reported using per mil (‰) notation relative to VPDB (Vienna Pee Dee Belemnite) for carbon, AIR for nitrogen, or VSMOW (Vienna Standard Mean Ocean Water) for oxygen, where ^aX is the heavier and ^bX is the lighter isotope ($^{13}\text{C}/^{12}\text{C}$, $^{15}\text{N}/^{14}\text{N}$, or $^{18}\text{O}/^{16}\text{O}$) for $\delta^{13}\text{C}_{\text{enamel}}$, $\delta^{15}\text{N}_{\text{enamel}}$, $\delta^{18}\text{O}_{\text{enamel}}$, and $\delta^{18}\text{O}_{\text{water}}$, respectively:

$$\delta^{a/b}\text{X} = \frac{(^a\text{X}/^b\text{X})_{\text{sample}}}{(^a\text{X}/^b\text{X})_{\text{standard}}} - 1$$

$\delta^{18}\text{O}_{\text{enamel}}$ values were converted from VPDB into VSMOW after Coplen (1988).

Nitrogen isotopes in tooth enamel

All living organisms require nitrogen as a major nutrient, which animals acquire from the food they consume (Ambrose and Norr, 1993). Due to isotopic fractionation during metabolism and subsequent excretion of waste, a consumer's $^{15}\text{N}/^{14}\text{N}$ ratio is elevated compared to their diet. As a result, animals typically have $\delta^{15}\text{N}$ tissue values that are ca. 3–5‰ higher than the foods they consume (Figure 1; Schoeninger and DeNiro, 1984; Bocherens and Drucker, 2003; Fox-Dobbs et al., 2007; Krajcarz et al., 2018; Leichliter et al., 2021).

The living part of any terrestrial food web starts with plants (which in turn use energy from the sun). Most plants obtain nitrogen from the soil, and soil $\delta^{15}\text{N}$ systematically decreases with increasing mean annual precipitation and decreasing mean annual temperature (Evans, 2001; Robinson, 2001; Amundson et al., 2003). Soil $\delta^{15}\text{N}$ has an effect on the $\delta^{15}\text{N}$ values of plants (Codron et al., 2005) which in turn determines the $\delta^{15}\text{N}$ tissue values of primary and secondary consumers. Thus, climate influences the nitrogen isotope composition of animals living in a given ecosystem, which can vary across space and time (Ambrose, 1986, 1991; Ambrose and DeNiro, 1986). To avoid the confounding effects of regional baseline variability in nitrogen, we focus on the vertebrate community living in GNP. Our aim is to characterize the $\delta^{15}\text{N}_{\text{enamel}}$ values of herbivores (i.e., grazers, mixed-feeders, and browsers), omnivores, and carnivores living within this single and well-constrained ecosystem (Figure 2).

In addition to climate and habitat-driven baseline variation, digestive physiology and water dependence have also been proposed to affect the $\delta^{15}\text{N}$ of animals' tissues (Sealy et al., 1987; Ambrose, 1991; Hartman, 2010). For instance, studies suggest that the $\delta^{15}\text{N}$ values of ruminant herbivores differ from non-ruminants as the result of the incorporation of ^{15}N -enriched microbes community in their hindgut (Steinhour et al., 1982; Sutoh et al., 1987). Additionally, herbivore species with physiological adaptations for water conservation, such as the

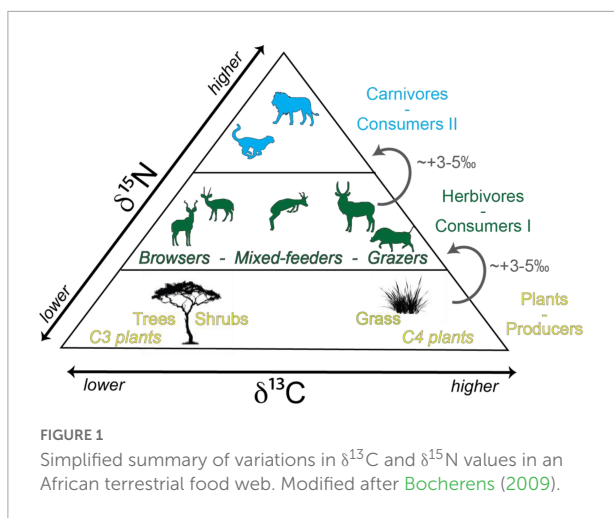
excretion of concentrated urine, are proposed to have higher $\delta^{15}\text{N}$ values than water-dependent animals (Ambrose, 1991 and references therein). However, the effects of digestive physiology and water dependence are still poorly understood and not well-tested (Ambrose, 1991; Cantalapiedra-Hijar et al., 2015). In this study, herbivorous ruminants and non-ruminants, as well as obligate drinkers and non-obligate drinkers were analyzed to evaluate these hypotheses.

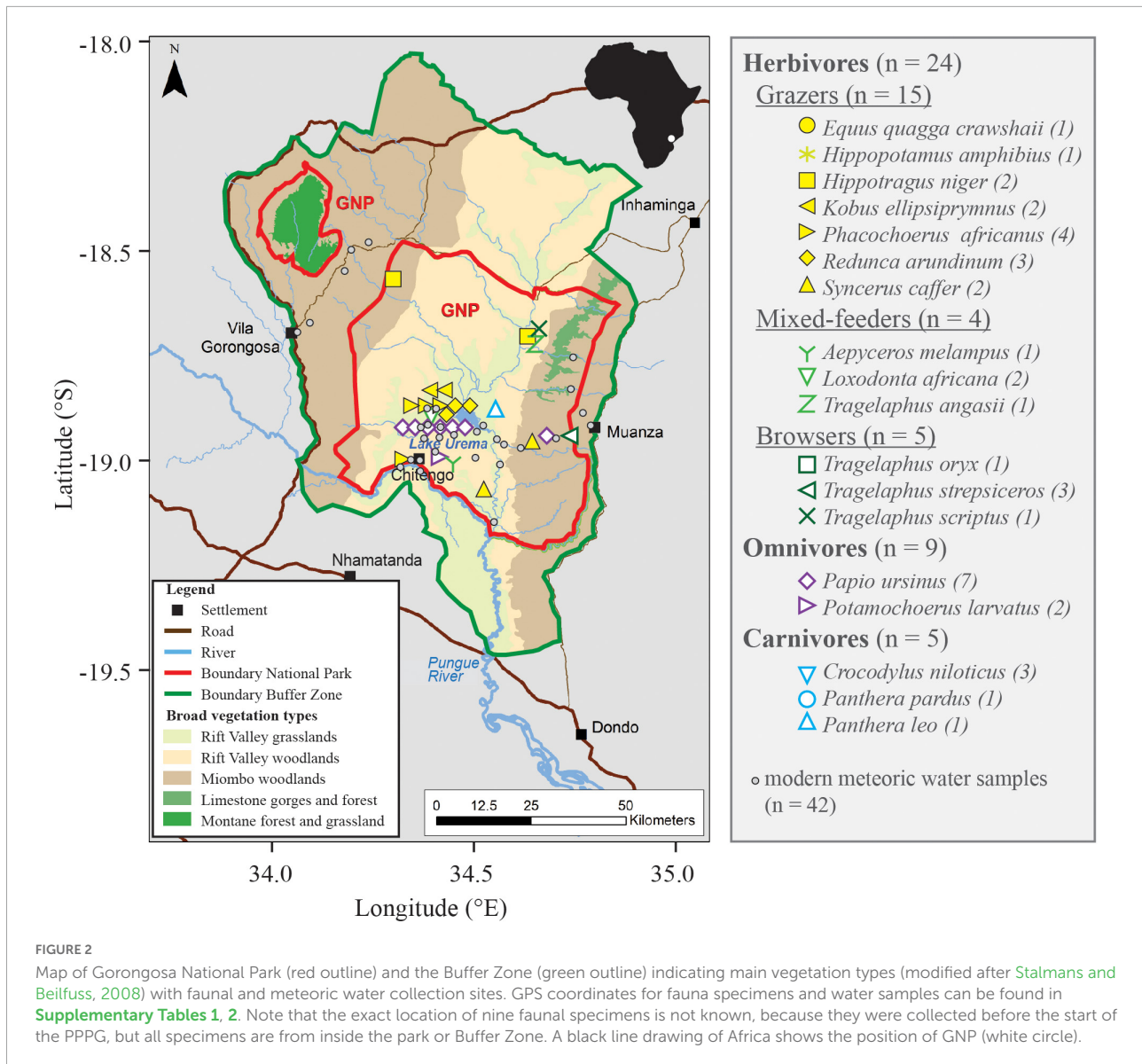
Carbon isotopes in tooth enamel

In contrast to $\delta^{15}\text{N}$, $\delta^{13}\text{C}$ of animal tissues increases only slightly with each step in the food chain (ca. 1‰ per trophic level; DeNiro and Epstein, 1981; Schoeninger and DeNiro, 1984; Bocherens and Drucker, 2003; O'Connell et al., 2012). In Africa, this signal is usually overprinted by the larger $\delta^{13}\text{C}$ differences between plants using different photosynthetic pathways; therefore, $\delta^{13}\text{C}_{\text{enamel}}$ cannot be reliably used for trophic-level reconstructions. However, $\delta^{13}\text{C}_{\text{enamel}}$ is a robust and well-established tool for reconstructing the plant-based diet of an animal (Figure 1; e.g., Cerling et al., 2015).

Dicots (trees, bushes, and herbs) use the C_3 photosynthetic pathway, whereas most tropical grasses and sedges use the C_4 photosynthetic pathway (e.g., Percy and Ehleringer, 1984). C_4 photosynthesis is advantageous in warm and seasonally dry, open environments with high light intensity, whereas the C_3 pathway is typically prevalent under low water stress and high- pCO_2 conditions (Kohn, 2010). Another pathway (Crassulacean Acid Metabolism; Wolf, 1960; Lüttge, 2004) is used by very arid-adapted plants like succulents, but these are rare at GNP and do not contribute significantly to the diet of the studied animals.

As a result of differential discrimination against $^{13}\text{CO}_2$ during photosynthesis, C_3 and C_4 types can be distinguished based on their $\delta^{13}\text{C}$ values (Figure 1). The $\delta^{13}\text{C}$ values of African C_4 plants range from -19‰ to -9‰ , while those of C_3 plants lie between -29‰ and -25‰ , resulting in bimodal and non-overlapping $\delta^{13}\text{C}$ values (Smith and Epstein, 1971; Percy and Ehleringer, 1984; Cerling et al., 2003; Kohn, 2010). Plant $\delta^{13}\text{C}$ values are reflected in the tissues of the animals that consume them, such that C_4 grazing ($>70\%$ C_4 grass consumption), mixed-feeding ($>30\%$ C_4 grass and $>30\%$ C_3 browse), and browsing ($>70\%$ C_3 browse) taxa can be differentiated (Cerling et al., 2003). Isotopic fractionation from diet to tooth takes place during enamel biomineralization. Large herbivore $\delta^{13}\text{C}_{\text{enamel}}$ values are enriched by ~ 14.5 to $12.0 \pm 1.0\text{‰}$ compared to the plants that they consume, depending on their digestive strategies (Cerling and Harris, 1999; Tejada-Lara et al., 2018; Cerling et al., 2021). Generally, browsers have $\delta^{13}\text{C}_{\text{enamel}}$ values lower than -8‰ , grazers have values above -2‰ , and values in between are typical for mixed-feeders (Cerling and Harris, 1999; Uno et al., 2018). Carnivore $\delta^{13}\text{C}_{\text{enamel}}$ values are determined by the isotopic composition of their prey, with negligible isotopic fractionation (Bocherens and Drucker, 2003).





Stable oxygen isotopes in tooth enamel and drinking water

The oxygen isotope composition of tooth enamel can be measured in either structural carbonate (CO_3) or phosphate (PO_4). Here, we report measurements on structural carbonate. For mammals, the $\delta^{18}\text{O}$ values of both components can be converted with the equation $\delta^{18}\text{O}_{\text{PO}_4} \approx 0.98 * \delta^{18}\text{O}_{\text{CO}_3} - 8.5$ after [Iacumin et al. \(1996\)](#). While reptiles may have a slightly different PO_4 to CO_3 relationship than mammals due to physiological effects ([Stanton and Carlson, 2004](#)), this has not been adequately studied to establish a separate equation for this group.

The oxygen isotope composition of tooth enamel is directly linked to the $\delta^{18}\text{O}$ values of body water which itself is a complex function of (micro)habitat, climate, diet, drinking behavior,

and physiology (e.g., [Bryant and Froelich, 1995](#); [Kohn, 1996](#); [Pederzani and Britton, 2019](#)). The body's main oxygen sources are drinking water, food, and atmospheric O_2 .

In sub-Saharan Africa, meteoric water (i.e., available drinking water) is often strongly influenced by the composition of the source water and evaporation processes (for details regarding GNP meteoric water, refer to the following section and [Steinbruch, 2010](#); [Steinbruch and Weise, 2014](#)). To interpret variability in $\delta^{18}\text{O}_{\text{enamel}}$ in the GNP fauna, we measured $\delta^{18}\text{O}$ of potential drinking water (i.e., permanent and ephemeral lakes and streams, rain, and groundwater, in the park and surrounding areas).

In warm-blooded mammals with an internally regulated body temperature (ca. 37°C for most mammals larger than 1 kg), biogenic hydroxyapatite is precipitated at a constant

temperature, and thus the oxygen isotopic signature of ingested food and water is recorded without temperature-dependent fractionation. For large herbivores, digested water is assumed to be equivalent to surficial water (Bryant and Froelich, 1995). There is an offset between $\delta^{18}\text{O}$ of body water and the $\delta^{18}\text{O}$ of the bioapatite (Bryant et al., 1996; Iacumin et al., 1996) according to the generalized equation for mammalian taxa of $\delta^{18}\text{O}_{\text{water}} \approx (\delta^{18}\text{O}_{\text{enamel(PO}_4)} - 23)/0.9$ (Kohn and Cerling, 2002); taxon-specific variations (refer to e.g., Ayliffe et al., 1992), relative humidity, and water temperature can, however, change this correlation (Kohn, 1996). The oxygen isotope compositions of *Crocodylus* correlate with those of ambient water according to the equation $\delta^{18}\text{O}_{\text{enamel(PO}_4)} \approx (\delta^{18}\text{O}_{\text{water}} + 19.13)/0.82$ (Amiot et al., 2007).

In additional consideration, African mammals can be divided into obligate and non-obligate drinkers. $\delta^{18}\text{O}_{\text{enamel}}$ of large-bodied (>100 kg), obligate drinkers have been shown to primarily reflect the $\delta^{18}\text{O}_{\text{water}}$ values of consumed water, and hence their $\delta^{18}\text{O}_{\text{enamel}}$ is closely related to the isotopic composition of their ambient environment (Bryant and Froelich, 1995; Kohn, 1996; Hoppe, 2006). However, non-obligate drinking animals, such as drought-adapted herbivores, obtain large proportions (or even all) of their water from the plant foods they consume (e.g., Nicholson, 1985). This behavior can lead to an increase in $\delta^{18}\text{O}_{\text{enamel}}$ values because leaf water is sensitive to evaporation, resulting in high $\delta^{18}\text{O}$ values in this part of the plant (Levin et al., 2006).

Additionally, plant $\delta^{18}\text{O}$ composition can vary as the result of differences in feeding behavior (e.g., $\delta^{18}\text{O}_{\text{enamel}}$ values typically decrease with increasing fraction of C_3 diet, because C_3 plants have lower $\delta^{18}\text{O}$ values than coexisting C_4 plants) (Bocherens et al., 1996).

At GNP, both obligate drinkers, which mostly include grazers and omnivores (e.g., hippos, equids, elephants, primates, suids), as well as non-obligate drinkers, mainly browsers and mixed-feeders (e.g., eland, bushbuck, kudu, nyala, and sable, refer to Cain et al., 2012), were sampled (refer to Table 1).

Materials and methods

Gorongosa National Park

Gorongosa National Park is located in the Sofala Province in central Mozambique (Figure 2) in the Urema Rift, the southernmost part of the East African Rift System. The unfenced park encompasses a 3,688 km² mosaic of diverse habitats and is surrounded by an inhabited “Buffer Zone” consisting mostly of agricultural lands (Figure 2). The valley floor is ca. 40 km wide and flanked to the east and west by hilly terrain rising to 400 m (Stalmans and Beilfuss, 2008; Stalmans et al., 2019). The region’s climate is influenced by the migration of the Intertropical Convergence Zone and is dominated by hot wet

summers and cooler dry winters with a mean annual rainfall of 700–900 mm. Over 80% of the annual rainfall occurs between November and March and is derived from the Indian Ocean, although some rainfall can also occur in the dry months as a result of the inflow of sub-polar mist cold air and continental compression (Steinbruch and Weise, 2014; Stalmans et al., 2019; Ma et al., 2021).

A central feature of the park is Lake Urema, which is on average only 2 m deep (Böhme, 2005) and is drained through a floodplain and the Urema River into the Pungwe River (Figure 2). The lake is fed by several ephemeral rivers that flow only in the wet season. In the dry season, the lake water infiltrates aquifer systems at the transition of the escarpments of the Urema Graben (Steinbruch, 2010; Arvidsson et al., 2011). The Lake Urema floodplain extends for >300 km² and floods annually (Steinbruch and Merkel, 2008), becoming uninhabitable for most terrestrial animals during the wet season. Stalmans and Beilfuss (2008) identified and mapped five major habitat types within GNP (Figure 2). From west to east, these are (i) Midlands miombo woodland (*Brachystegia* and *Julbernardia* sp.) on the western rim of the Rift Valley (331 km²); (ii) Alluvial Fan *Acacia*, *Combretum*, and palm savannas (1,265 km²); (iii) floodplain grasslands (759 km²) around Lake Urema; (iv) Colluvial Fan savannas (326 km²) within the Rift Valley; and (v) Cheringoma Plateau miombo woodlands and forested limestone gorges on the eastern rim of the Rift Valley (938 km²).

These landscapes have an overall proportional tree cover of 0.39 (Daskin et al., 2016) and support a large diversity of herbivores, including grazers, browsers, and mixed-feeders (Tinley, 1977; Stalmans and Beilfuss, 2008; Daskin et al., 2016; Stalmans et al., 2019; Gaynor et al., 2021). However, while Gorongosa was once renowned for its large mammal population (Tinley, 1977), the ecosystem experienced severe perturbation during 15 years of civil war (1977–1992), from which it is still recovering today. Most apex predators were extirpated from the park during this time, including leopards, African wild dogs, and spotted hyenas. Of these taxa, leopards have recently re-colonized the Buffer Zone by migrating from surrounding areas, and five additional adult leopards as well as two founding packs of wild dogs have been re-introduced from different regions in South Africa (Bouley et al., 2021). Lions and crocodiles are the only apex predators that persisted throughout the periods of war and recovery; however, the lions’ abundance was greatly reduced (Pringle, 2017; Bouley et al., 2018). Herbivore populations were similarly decimated. Before the war, elephants, hippos, buffalo, zebra, and wildebeest dominated the herbivore fauna but today are outnumbered by waterbuck and other small to mid-size antelopes (Stalmans et al., 2019).

The Gorongosa Restoration Project, established in 2006, is focused on long-term biodiversity conservation, sustainable development of the neighboring Buffer Zone, training farmers in new practices to improve crop yields, and improving the health and education of communities in the greater Gorongosa

TABLE 1 List of all 38 analyzed specimens including diet, common and Latin name, catalog ID, and stable nitrogen, carbon, and oxygen values in ‰ and nitrogen content. Mean values for each dietary group are shown in bold.

Diet	Common name	Taxon	Catalog ID	$\delta^{15}\text{N}_{\text{enamel}}$ (‰ vs. AIR)	$\delta^{13}\text{C}_{\text{enamel}}$ (‰ vs. VPDB)	$\delta^{18}\text{O}_{\text{enamel}}$ (‰ vs. VSMOW)	N content (nmol/mg)
Grazing	Buffalo	<i>Syncerus caffer</i>	PPG2017-B-19	4.3 ± 0.3 (3)	1.5 ± 0.1 (2)	30.4 ± 0.3 (2)	7.9 ± 2.0 (3)
	Buffalo	<i>Syncerus caffer</i>	PPG2017-B-41	7.6 ± 0.0 (2)	-2.1 ± 0.3 (2)	28.9 ± 0.2 (2)	3.4 ± 0.3 (2)
	Hippo	<i>Hippopotamus amphibius</i>	PPG2016-B-07	7.6 ± 0.4 (2)	-4.0 ± 0.1 (2)	26.2 ± 0.0 (2)	3.7 ± 0.0 (2)
	Reedbuck	<i>Redunca arundinum</i>	PPG2016-B-27	3.6 ± 0.6 (2)	0.5 ± 0.0 (2)	31.4 ± 0.3 (2)	6.8 ± 1.0 (2)
	Reedbuck	<i>Redunca arundinum</i>	PPG2017-B-17	4.7 ± 0.3 (2)	0.6 ± 0.2 (3)	31.4 ± 0.2 (3)	6.1 ± 0.7 (2)
	Reedbuck	<i>Redunca arundinum</i>	PPG2017-B-59	4.7 ± 0.3 (2)	0.3 ± 0.0 (2)	33.1 ± 0.2 (2)	5.7 ± 0.1 (2)
	Sable	<i>Hippotragus niger</i>	PPG-B-01	4.8 ± 0.1 (2)	1.2 ± 0.0 (2)	31.3 ± 0.0 (2)	5.9 ± 0.9 (2)
	Sable	<i>Hippotragus niger</i>	PPG2017-B-47	5.9 ± 0.0 (2)	1.8 ± 0.1 (2)	32.7 ± 0.2 (2)	3.6 ± 0.1 (2)
	Warthog	<i>Phacochoerus africanus</i>	PPG2017-B-30	6.3 ± 0.4 (2)	-1.9 ± 0.4 (2)	29.3 ± 0.3 (2)	3.8 ± 0.8 (2)
	Warthog	<i>Phacochoerus africanus</i>	PPG2017-B-04	5.9 (1)	-3.8 ± 0.3 (2)	28.7 ± 0.3 (2)	4.7 (1)
	Warthog	<i>Phacochoerus africanus</i>	PPG2016-B-25	5.5 ± 0.1 (2)	-2.7 ± 0.1 (2)	30.1 ± 0.3 (2)	4.7 ± 1.7 (2)
	Warthog	<i>Phacochoerus africanus</i>	PPG2017-B-29	5.1 ± 0.2 (2)	-1.3 ± 0.6 (2)	31.8 ± 0.6 (2)	4.9 ± 0.4 (2)
	Waterbuck	<i>Kobus ellipsiprymnus</i>	PPG2016-B-15	7.5 ± 0.3 (2)	0.6 ± 0.1 (2)	32.7 ± 0.2 (2)	4.8 ± 0.0 (2)
	Waterbuck	<i>Kobus ellipsiprymnus</i>	PPG2016-B-24	7.9 ± 0.1 (2)	-4.3 ± 0.0 (3)	31.1 ± 0.5 (3)	4.9 ± 0.3 (2)
	Zebra	<i>Equus quagga crawshaii</i>	PPG-B-02	6.9 (1)	-3.3 ± 0.0 (2)	29.1 ± 0.5 (2)	2.2 (1)
	Grazers mean values (n = 15)				5.9 ± 1.4	-1.1 ± 2.2	30.5 ± 1.9
Mixed-feeding	Elephant	<i>Loxodonta africana</i>	PPG-B-08	7.3 ± 0.2 (2)	-10.7 ± 0.1 (2)	28.9 ± 0.1 (2)	6.0 ± 0.6 (2)
	Elephant	<i>Loxodonta africana</i>	PPG-B-03	8.1 ± 0.2 (2)	-10.5 ± 0.1 (2)	29.8 ± 0.3 (2)	5.8 ± 1.5 (2)
	Impala	<i>Aepyceros melampus</i>	PPG2017-B-28	7.0 ± 0.4 (3)	-3.6 ± 0.0 (2)	29.8 ± 0.3 (2)	4.8 ± 0.8 (3)
	Nyala	<i>Tragelaphus angasii</i>	PPG2017-B-45	4.5 ± 0.2 (2)	-14.8 ± 0.1 (4)	31.4 ± 0.1 (4)	4.8 ± 0.2 (2)
Mixed-feeders mean values (n = 4)				6.7 ± 1.6	-9.9 ± 4.7	30.0 ± 1.1	5.4 ± 0.6
Browsing	Bushbuck	<i>Tragelaphus scriptus</i>	PPG2017-B-44	7.2 ± 0.1 (2)	-11.8 ± 0.0 (2)	31.9 ± 0.0 (2)	6.7 ± 2.0 (2)
	Eland	<i>Tragelaphus oryx</i>	PPG2017-B-31	4.5 ± 0.0 (2)	-14.7 ± 0.1 (2)	31.2 ± 0.2 (2)	4.9 ± 0.1 (2)
	Greater Kudu	<i>Tragelaphus strepsiceros</i>	PPG-B-04	6.1 ± 0.1 (2)	-15.1 ± 0.2 (2)	31.2 ± 0.4 (2)	4.4 ± 0.5 (2)
	Greater Kudu	<i>Tragelaphus strepsiceros</i>	PPG-B-05	5.9 ± 0.2 (2)	-14.4 ± 0.2 (2)	30.5 ± 0.2 (2)	4.0 ± 0.2 (2)
	Greater Kudu	<i>Tragelaphus strepsiceros</i>	PPG2017-B-58	3.8 ± 0.0 (2)	-15.8 ± 0.1 (2)	29.9 ± 0.3 (2)	3.8 ± 0.4 (2)
Browsers mean values (n = 5)				5.5 ± 1.5	14.3 ± 1.5	31.0 ± 0.8	4.8 ± 1.2
All herbivores mean values (n = 24)				5.9 ± 1.4	-5.4 ± 6.2	30.5 ± 1.2	4.9 ± 1.3
Omnivorous	Bushpig	<i>Potamochoerus larvatus</i>	PPG2017-B-32	4.5 ± 0.2 (2)	-13.7 ± 0.0 (2)	26.0 ± 0.2 (2)	8.3 ± 1.2 (3)
	Bushpig	<i>Potamochoerus larvatus</i>	PPG2017-B-25	6.2 ± 0.6 (3)	-9.5 ± 0.0 (2)	28.4 ± 0.0 (2)	3.6 ± 0.2 (2)
	Baboon	<i>Papio ursinus</i>	PPG2016-B-05	4.6 ± 0.4 (3)	-12.78 ± 0.0 (2)	30.5 ± 0.2 (2)	3.5 ± 0.4 (2)
	Baboon	<i>Papio ursinus</i>	PPG2018-B-28	2.2 ± 0.2 (2)	-13.1 ± 0.2 (3)	28.4 ± 0.3 (3)	4.9 ± 0.7 (2)
	Baboon	<i>Papio ursinus</i>	PPG2017-B-34	5.5 ± 0.5 (2)	-8.2 ± 0.3 (2)	28.9 ± 0.3 (2)	4.6 ± 0.3 (2)
	Baboon	<i>Papio ursinus</i>	PPG2016-B-10	3.9 ± 0.2 (2)	-7.9 ± 0.0 (2)	28.5 ± 0.2 (2)	4.8 ± 1.1 (2)
	Baboon	<i>Papio ursinus</i>	PPG2016-B-16	6.3 ± 0.3 (2)	-8.4 ± 0.2 (3)	29.2 ± 0.1 (3)	3.9 ± 0.3 (2)
	Baboon	<i>Papio ursinus</i>	PPG2016-B-20	5.9 ± 0.4 (2)	-11.7 ± 0.3 (3)	29.0 ± 0.4 (3)	2.0 ± 0.1 (2)
	Baboon	<i>Papio ursinus</i>	PPG2017-B-28	6.6 ± 0.2 (2)	-9.9 ± 0.1 (3)	28.5 ± 0.3 (3)	2.5 ± 0.2 (3)
Omnivores mean values (n = 9)				5.1 ± 1.4	-10.6 ± 2.3	28.6 ± 1.2	4.2 ± 1.8
Carnivorous	Leopard	<i>Panthera pardus</i>	PPG2019-B-09	7.2 ± 0.3 (2)	-11.0 ± 0.0 (2)	28.1 ± 0.3 (2)	4.0 ± 0.2 (2)
	Lion	<i>Panthera leo</i>	PPG2018-B-02	12.3 ± 0.2 (2)	-8.1 ± 0.3 (3)	29.9 ± 0.5 (3)	4.0 ± 0.4 (2)
	Crocodile	<i>Crocodylus niloticus</i>	PPG2016-B-39	10.9 ± 0.4 (2)	-6.4 ± 0.2 (2)	27.1 ± 0.2 (2)	9.7 ± 1.0 (2)
	Crocodile	<i>Crocodylus niloticus</i>	PPG2016-B-38	9.3 ± 0.3 (3)	-6.9 ± 0.1 (2)	27.2 ± 0.5 (2)	8.4 ± 1.5 (3)
	Crocodile	<i>Crocodylus niloticus</i>	PPG-B-06	10.0 ± 0.1 (2)	-3.1 ± 0.3 (2)	29.0 ± 0.0 (2)	10.6 ± 1.2 (2)
Carnivores mean values (n = 5)				9.9 ± 1.9	-7.1 ± 2.9	28.3 ± 1.2	7.4 ± 3.1

The number of analyses, typically duplicate, is given in brackets.

region. Due to these efforts, the GNP ecosystem is slowly recovering and offers a unique setting in which to study the adaptation of mammals to dynamic and complex environments. Today, numerous projects are underway in GNP. These studies use a combination of methods including motion-triggered cameras (Gaynor et al., 2018, 2021; Easter et al., 2019), biologgers (often including Global Positioning System units, triaxial accelerometers, and sometimes video recorders; e.g., Branco et al., 2019a,b; Becker et al., 2021; Bouley et al., 2021), aerial counts (Cumming et al., 1994; Dutton and Carvalho, 2002; Dunham, 2004; Stalmans, 2012; Stalmans et al., 2019), animal follows (Hammond et al., 2022), molecular studies (Martinez et al., 2019; Santander et al., 2022), and other field observation tools (e.g., Muschinski et al., 2019) to gain insights in the park's ecology. The $\delta^{13}\text{C}_{\text{enamel}}$, $\delta^{15}\text{N}_{\text{enamel}}$, and $\delta^{18}\text{O}_{\text{enamel}}$ datasets of Gorongosa's fauna presented here—the first stable isotopes result for any terrestrial fauna in Mozambique—will help us to better understand dietary patterns of the large-bodied animals which roam GNP today.

Material and sampling protocol

Tooth enamel

Since 2016, remains of modern fauna have been collected from different regions of the park and the surrounding Buffer Zone (Figure 2 and Supplementary Table 1) by members of the Paleo-Primate Project Gorongosa (PPPG). We selected as many different vertebrate taxa as possible and analyzed the tooth enamel of 38 adult individuals (17 mammalian taxa and one reptile; refer to Table 1) for organic $\delta^{15}\text{N}_{\text{enamel}}$ as well as inorganic $\delta^{13}\text{C}_{\text{enamel}}$ and $\delta^{18}\text{O}_{\text{enamel}}$. These include 15 grazers, four mixed-feeders, five browsers, nine omnivores, and five carnivores. The bone weathering stage was 0–1, suggesting that all animals died within the last few years prior to field collection (after Behrensmeyer, 1978).

During sampling, the topmost ca. 0.2 mm of enamel was discarded to avoid contamination by any adherent sediment. Tooth enamel powder was sampled using a Dremel handheld drill with a diamond ball head drill tip (0.9 mm diameter) at low to medium speed (1,000–2,000 RMP). For herbivore specimens, which generally have thick enamel, the sampling depth was 0.5–1 mm. For carnivores and some omnivores which have only a thin layer of enamel, great care was taken to avoid the underlying dentin, and sampling was conducted to a shallower depth, over a larger area of the tooth. Bulk enamel samples were usually taken longitudinally, between the cusp and the cervix, integrating at least 3 months of the dietary signal. We collected 10–50 mg of enamel for carbon, nitrogen, and oxygen isotope analyses, which were measured in duplicate or triplicate whenever possible.

Meteoric water

Water samples from the lake ($n = 15$), river ($n = 18$), rain ($n = 4$), and groundwater ($n = 5$) sources were collected

from GNP and the surrounding Buffer Zone between 2016 and 2019 (Figure 2 and Supplementary Table 2) in both dry seasons (May to October; $n = 32$; mostly permanent lakes and rivers, groundwater) and wet season (November to April; $n = 10$; rainwater, ephemeral and permanent lakes/water holes, floodplain). These water sources represent potential drinking water for the Gorongosa fauna.

At each sampling site, 30 ml of unfiltered water was collected with as little air volume as possible in high-density polyethylene bottles. Rainwater was captured directly from the runoff of an aluminum roof at Camp Chitengo (Figure 2). Groundwater was sampled from water pumps which were run for at least 3 min prior to sampling. Samples were stored at room temperature and in the dark until returned to the laboratory for refrigeration and subsequent analysis.

Analyses

Nitrogen isotope analysis of tooth enamel using a novel "oxidation-denitrification method"

We use the "oxidation-denitrification method" to measure the $\delta^{15}\text{N}_{\text{enamel}}$ of mineral-bound nitrogen in tooth enamel at the Max Planck Institute for Chemistry (MPIC). The "oxidation-denitrification method" was first used for marine-dissolved organic nitrogen (Knapp et al., 2005) and marine microfossil-bound nitrogen (Robinson et al., 2004; Ren et al., 2009). The protocol used here for enamel-bound nitrogen follows Leichliter et al. (2021). It includes reductive-oxidative cleaning of enamel powder followed by oxidation of enamel-bound organic matter to nitrate using a basic solution of potassium peroxydisulfate in a specially designed clean room. Nitrate is subsequently converted to N_2O using the bacteria *Pseudomonas chlororaphis*, grown, cultured, and harvested at the MPIC following the methods outlined by Sigman et al. (2001) and Weigand et al. (2016). The isotopic composition of the N_2O is extracted, purified, and analyzed by an automated purge-trap, gas chromatography-isotope ratio mass spectrometry, in this case by a custom-built system online to a Thermo Scientific MAT253-Plus isotope ratio mass spectrometer (Weigand et al., 2016). Coupled with the denitrification step for N_2O production, this system results in high-precision measurements ($1\sigma < 0.1\text{‰}$) of nitrogen isotopes of nitrate down to 5 nmol N (Weigand et al., 2016).

We cleaned and measured each sample (5–7 mg of enamel powder) in duplicate or triplicate (exceptions are PPG-B-02 and PPG2017-B-04 due to limited sample amounts) in different batches, resulting in 78 individual measurements in five different batches.

Individual nitrate isotopic analyses are referenced to injections of N_2O and standardized using international nitrate reference materials IAEA-NO3 and USGS34. Additionally,

sample data were corrected for the contribution of the blank using the nitrogen content and $\delta^{15}\text{N}$ values of oxidation blanks after Leichliter et al. (2021). Blank N content was between 0.3 and 0.4 nmol/ml, resulting in an average blank contribution of 3% or less. Inter-batch precision ($\pm 1\sigma$) in $\delta^{15}\text{N}$ for international standards is $<0.2\text{‰}$ for USGS65 (glycine; $n = 7$); $<0.3\text{‰}$ for USGS 40 (L-glutamic acid; $n = 16$); and $<0.4\text{‰}$ for USGS41 (L-glutamic acid; $n = 11$; **Supplementary Table 3**). For in-house standards (refer to Leichliter et al., 2021), this precision is $<0.4\text{‰}$ for coral standard PO-1 (*Porites* sp.; $n = 18$) and LO-1 (*Lophelia pertusa*; $n = 17$) and $<0.5\text{‰}$ for tooth enamel standards AG-Lox (modern *Loxodonta africana*; $n = 18$) and Noto-1 (Late-Pleistocene *Notochoerus scotti*; $n = 17$), across all analytical batches (**Supplementary Table 4**).

Stable carbon and oxygen isotope analyses of tooth enamel

High-precision stable carbon and oxygen isotope analysis of small sample amounts (~ 50 – 100 μg of untreated enamel) was performed using the “cold trap method” (Vanhof et al., 2020a) at the laboratories of the Climate Geochemistry Department at MPIC in Mainz, Germany. We used a Thermo Delta-V mass spectrometer in continuous flow configuration, directly interfaced with a GasBench II gas preparation unit with an integrated pneumatically operated cold trap system. In automated mode, digestion of enamel occurs in 12 ml He-flushed exetainer vials with $>99\%$ H_3PO_4 at 70°C for 90 min. Then, the CO_2 sample is carried with ultrapure He to the cold trap where it is cryogenically focused for 6–7 min by cooling the trap with liquid N_2 . After lifting the trap out of the liquid N_2 , the carrier gas with the sample CO_2 passes through a standard Poraplot-Q Gas Chromatography (GC) column where the entire CO_2 sample is delivered to the mass spectrometer for carbon and oxygen isotope analyses in a single peak, preceded by five reference gas peaks. Calculation of isotope values follows Vanhof et al., 2020a,b with the international standards IAEA-603, NBS18, and/or NBS120c in addition to two internal house standards: a carbonate standard (VICs) and tooth enamel standard AG-Lox, the latter was also used as a standard for $\delta^{15}\text{N}_{\text{enamel}}$ for reference (**Supplementary Table 5**). Overall analytical uncertainties are better than 0.09‰ for $\delta^{13}\text{C}_{\text{enamel}}$ and 0.14‰ for $\delta^{18}\text{O}_{\text{enamel}}$ (1σ standard deviation of AG-Lox within batches). Carbonate contents were derived from standard vs. sample total peak area ratios (7.5% structural carbonate content for AG-Lox; after Vanhof et al., 2020b).

Oxygen isotope analyses of meteoric waters

Oxygen isotope ratios were measured on 1 ml aliquots using an LGR 24d liquid water isotope analyzer at the Goethe University-Senckenberg BiK-F Joint Stable Isotope Facility, Frankfurt, Germany (Schemmel et al., 2013). The $\delta^{18}\text{O}_{\text{water}}$ values are calibrated and reported against VSMOW, with an analytical precision of $<0.2\text{‰}$ (2σ).

Statistical analyses

Statistical analyses of elemental content and univariate isotope values were performed using Paleontological Statistics (PAST4) version 4 (Hammer et al., 2001). Statistical significance between isotopic groups was determined using one-way ANOVA with a Tukey–Kramer HSD *post hoc* test if not stated otherwise with a level of significance of $p = 0.050$. Pearson correlation coefficient (r) is given for correlations.

Statistical analyses of multivariate isotope comparisons were performed in R (version 4.2.0; R Core Team, 2022). Isotopic niches were analyzed using the Stable Isotopes Bayesian Ellipses (SIBER) package (version 2.1.6; Jackson et al., 2011) and the Turner et al. (2010) statistical code. Data normality was first checked using the Shapiro–Wilk test for both individual groups by element using the *nor.test* function from the *onewaytests* package (Dag et al., 2018), and with a multivariate Shapiro–Wilk test for the entire dataset using the *mshapiro_test* function from the *rstatix* package (Kassambra, 2021). Data normality was assumed if $p > 0.050$ for all tests. The isotopic niches of the four different *a priori* dietary groups with $n \geq 5$ were determined by fitting their distribution of $\delta^{13}\text{C}_{\text{enamel}}$, $\delta^{15}\text{N}_{\text{enamel}}$, and $\delta^{18}\text{O}_{\text{enamel}}$ isotope values with estimated standard ellipse areas corrected for sample size (SEA_C ; Jackson et al., 2011). The SEA_C contains 40% of the variation of a group and was chosen over SEA as it limits calculation biases due to small and unbalanced sample sizes and is appropriate when the analyzed groups contain fewer than 30 individuals (Syväranta et al., 2013; Pinzone et al., 2019). However, the mixed feeding group was not included in the multivariate analyses because of its sample size ($n = 4$) which does not meet the minimum sampling requirements for SEA_C as recommended by Jackson et al. (2011). Its mean value, standard deviation, and convex hull were still calculated and plotted for visual comparisons.

Geometric overlap between ellipses was calculated and compared between analyzed groups, both in total overlap (in ‰^2) and in proportional overlap (Jackson et al., 2011; refer to **Supplementary Tables 6–8**). Niche standard ellipse areas for each group were further explored using Bayesian modeling (SEA_B) and 50, 75, and 95% credible intervals were calculated and compared across groups. Finally, to determine whether the location of each group’s niche differed in isotopic space, the Euclidean distance between the centroids of each group was calculated and compared in pairs. A residual permutation procedure and Hotelling T^2 test were used to evaluate significance, with $p < 0.050$ indicating that the two compared niches occupy significantly different areas in isotopic space (Turner et al., 2010).

Results

We report $\delta^{15}\text{N}_{\text{enamel}}$, $\delta^{13}\text{C}_{\text{enamel}}$, $\delta^{18}\text{O}_{\text{enamel}}$, and N content data from 35 mammals and three reptiles sampled

in GNP, and the results are given in **Table 1**. For calculated $\delta^{18}\text{O}_{\text{drinking-water}}$, carbonate contents, tooth position, sex, GPS coordinates, and collection date and locality (habitat), refer to **Supplementary Table 1**. Additionally, we report $\delta^{18}\text{O}_{\text{water}}$ data from 42 meteoric water samples, results with water type (rain, river, lake, and groundwater), GPS coordinates, elevation, and collection date are given in **Supplementary Table 2**.

Nitrogen isotope values

$\delta^{15}\text{N}_{\text{enamel}}$ values of all 38 specimens range from 2.2 to 12.3‰, with mean $\delta^{15}\text{N}_{\text{enamel}}$ values of $5.9 \pm 1.4\text{‰}$ ($n = 24$) for herbivores, $5.1 \pm 1.4\text{‰}$ ($n = 9$) for omnivores, and $9.9 \pm 1.9\text{‰}$ ($n = 5$) for carnivores (**Figure 3A**). Carnivore nitrogen isotope ratios differ significantly from herbivores and omnivores ($p < 0.001$), while the $\delta^{15}\text{N}_{\text{enamel}}$ values of omnivores (bushpigs and baboons) do not differ significantly from herbivores ($p = 0.324$). Grazers ($6.9 \pm 1.4\text{‰}$, $n = 15$), mixed-feeders ($6.7 \pm 1.6\text{‰}$, $n = 4$), and browsers ($5.5 \pm 1.3\text{‰}$, $n = 5$) show no significant difference in their $\delta^{15}\text{N}_{\text{enamel}}$ values ($p = 0.428$). Herbivore taxa do not display significantly different $\delta^{15}\text{N}_{\text{enamel}}$ values when grouped according to digestive physiology ($p = 0.104$) or water dependency ($p = 0.128$; **Figure 4A**).

Nitrogen content in tooth enamel

The nitrogen content of clean tooth enamel ranges from 2.0 to 10.6 nmol/mg with an average of 5.1 ± 1.9 nmol/mg (**Figure 5** and **Table 1**). No significant correlation is observed between $\delta^{15}\text{N}_{\text{enamel}}$ and nitrogen content ($r = 0.285$; $p = 0.083$; **Figure 5A**). Carnivores have slightly higher N contents compared to the other dietary groups ($p = 0.008$). However, this difference is entirely driven by the high nitrogen content of crocodile enamel, and crocodiles were the only reptiles sampled (**Figure 5B**). No other differences in the N content of tooth enamel were observed between dietary groups.

Carbon isotope values

The complete range of C_3 to C_4 $\delta^{13}\text{C}$ values is represented in the Gorongosa fauna. $\delta^{13}\text{C}_{\text{enamel}}$ values range from -15.7 to 1.8‰ , with mean $\delta^{13}\text{C}_{\text{enamel}}$ values for herbivores of $-5.4 \pm 6.2\text{‰}$ ($n = 24$), $-10.6 \pm 21.4\text{‰}$ ($n = 9$) for omnivores, and $-7.1 \pm 2.9\text{‰}$ ($n = 5$) for carnivores. $\delta^{13}\text{C}_{\text{enamel}}$ values for grazing herbivores (mean = $-1.1 \pm 2.2\text{‰}$; $n = 15$), mixed-feeders ($-9.9 \pm 4.7\text{‰}$, $n = 4$), and browsers ($-14.3 \pm 1.5\text{‰}$; $n = 5$) are significantly different ($p < 0.001$). Herbivores

do not display significant differences in $\delta^{13}\text{C}_{\text{enamel}}$ values when grouped according to digestive physiology [ruminant ($n = 16$) vs. non-ruminant ($n = 8$); $p = 0.761$]. Herbivorous obligate drinkers ($n = 16$) have higher $\delta^{13}\text{C}_{\text{enamel}}$ values compared to non-obligate drinkers ($n = 8$; $p = 0.002$; **Figure 4B**).

The structural carbonate component of enamel powder ranges from 3 to 9% (**Supplementary Table 1**) with a mean of $6 \pm 1\%$. Herbivores have slightly higher carbonate content than omnivores ($p < 0.001$), while the other dietary groups do not differ ($p > 0.050$).

Oxygen isotope values

The $\delta^{18}\text{O}_{\text{enamel}}$ values for the Gorongosa fauna range from 26.0 to 33.1‰ with mean values of $30.5 \pm 1.6\text{‰}$ ($n = 24$) for herbivores, $28.6 \pm 1.2\text{‰}$ ($n = 9$) for omnivores, and $28.3 \pm 1.2\text{‰}$ for carnivores ($n = 5$). Herbivores differ statistically from other dietary groups ($p < 0.008$), while carnivores and omnivores are similar ($p = 0.907$). Ruminant $\delta^{18}\text{O}_{\text{enamel}}$ values are significantly higher than those of non-ruminants ($p < 0.001$). $\delta^{18}\text{O}_{\text{enamel}}$ values for herbivorous non-obligate drinkers are not significantly different than those of obligate drinkers ($p = 0.108$; **Figure 4C**).

The $\delta^{18}\text{O}_{\text{water}}$ values of drinking water range from -6.2 to 13.1‰ with a mean value of $-0.8 \pm 5.3\text{‰}$ ($n = 42$; **Figure 6** and **Supplementary Table 2**). Groundwaters have the lowest $\delta^{18}\text{O}_{\text{water}}$ values with an average of $-5.2 \pm 0.6\text{‰}$ ($n = 5$), followed by waters sampled from rivers ($-3.4 \pm 1.8\text{‰}$; $n = 18$), rainfall ($-2.5 \pm 1.3\text{‰}$; $n = 4$), and lakes ($4.1 \pm 6.1\text{‰}$; $n = 15$); this difference is statistically significant only when comparing lake water to samples from other reservoirs ($p < 0.020$). Lake $\delta^{18}\text{O}_{\text{water}}$ values sampled in the wet season (-4.9 to -1.5‰ ; mean = $-3.2 \pm 1.4\text{‰}$, $n = 5$) are significantly ($p < 0.001$) lower than dry season data (2.9 – 13.1‰ ; mean = $7.8 \pm 3.4\text{‰}$; $n = 10$), and there is no overlap in these two datasets.

Isotope niche analyses

Isotopic niche overlap, niche area, and distinction of niche space differed depending on the pairing of isotope values analyzed (**Figure 7** and **Supplementary Tables 6–8**). We could not reject the null hypotheses for all Shapiro–Wilks tests indicating data were normal for both the individual feeding group by element (all groups $p > 0.050$) as well as the entire multivariate dataset ($p = 0.212$).

For $\delta^{13}\text{C}_{\text{enamel}}$ vs. $\delta^{15}\text{N}_{\text{enamel}}$, there is no SEA_{C} overlap present (**Figure 7A**), and the Bayesian modes of niche size ranged from 4.0 to 13.1‰^2 with no statistical differences based on 95% credible intervals (**Figure 7B**). All dietary groups were statistically distinct in isotopic space ($p < 0.035$).

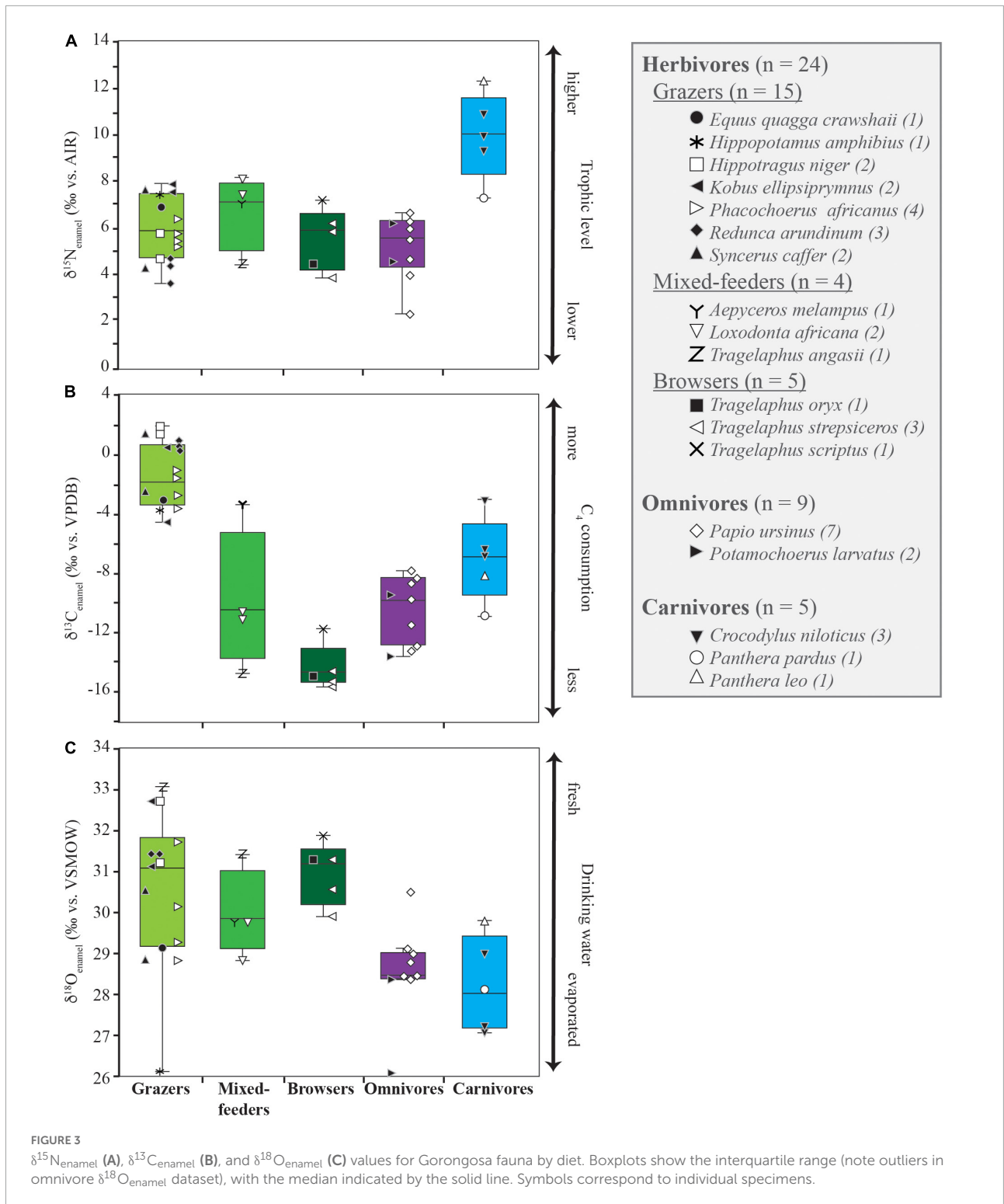
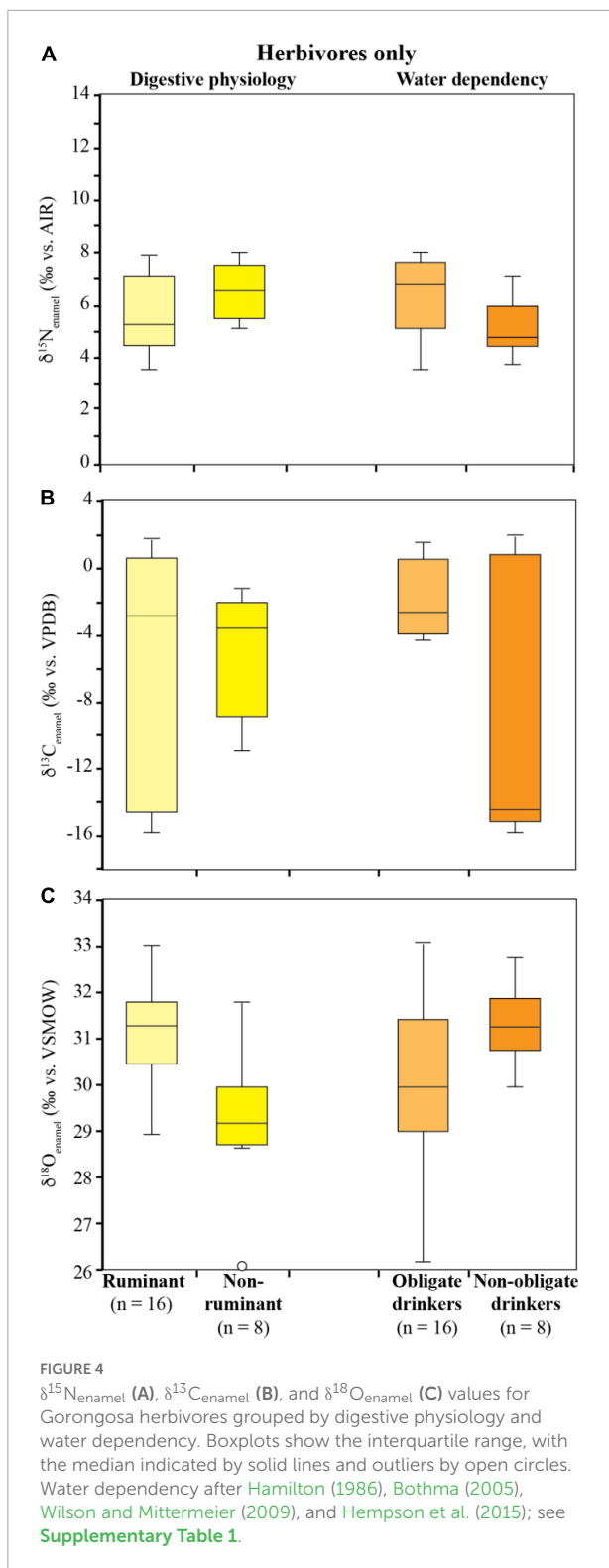


FIGURE 3
 $\delta^{15}\text{N}_{\text{enamel}}$ (A), $\delta^{13}\text{C}_{\text{enamel}}$ (B), and $\delta^{18}\text{O}_{\text{enamel}}$ (C) values for Gorongosa fauna by diet. Boxplots show the interquartile range (note outliers in omnivore $\delta^{18}\text{O}_{\text{enamel}}$ dataset), with the median indicated by the solid line. Symbols correspond to individual specimens.

For $\delta^{18}\text{O}_{\text{enamel}}$ vs $\delta^{15}\text{N}_{\text{enamel}}$, SEAC overlap ranged from 0 to 78%, and the Bayesian modes of niche size ranged from 2.2 to 7.2‰² with no statistical differences based on 95% credible intervals (Figure 7C). Isotopic niches were indistinct between grazers and browsers ($p = 0.790$) and were nearly

indistinct between browsers and omnivores ($p = 0.048$). All other dietary groups were statistically distinct in isotopic space when compared to one another ($p < 0.010$).

For $\delta^{13}\text{C}_{\text{enamel}}$ vs. $\delta^{18}\text{O}_{\text{enamel}}$, SEAC overlap ranged from 0 to 30% (Figure 7E), and the Bayesian modes of niche size



ranged from 2.4 to 9.1‰² with no statistical differences based on 95% credible intervals (Figure 7F). All dietary groups were statistically distinct in $\delta^{13}\text{C}_{\text{enamel}}$ vs $\delta^{18}\text{O}_{\text{enamel}}$ space when compared to one another ($p < 0.020$).

Sample sizes for some groups analyzed could affect calculated niche values. Small sample sizes (i.e., ~5) have been shown to underrepresent ellipse area (Jackson et al., 2011) and increase niche size uncertainty (Syväranta et al., 2013), although SEA_C aims to minimize this (Jackson et al., 2011). Increased replication could possibly change the niche overlap, shape, and areas of dietary groups. However, SEA_B accounts for this variability in its credible intervals, and the Turner et al. (2010) analysis of centroid position remains statistically valid.

Discussion

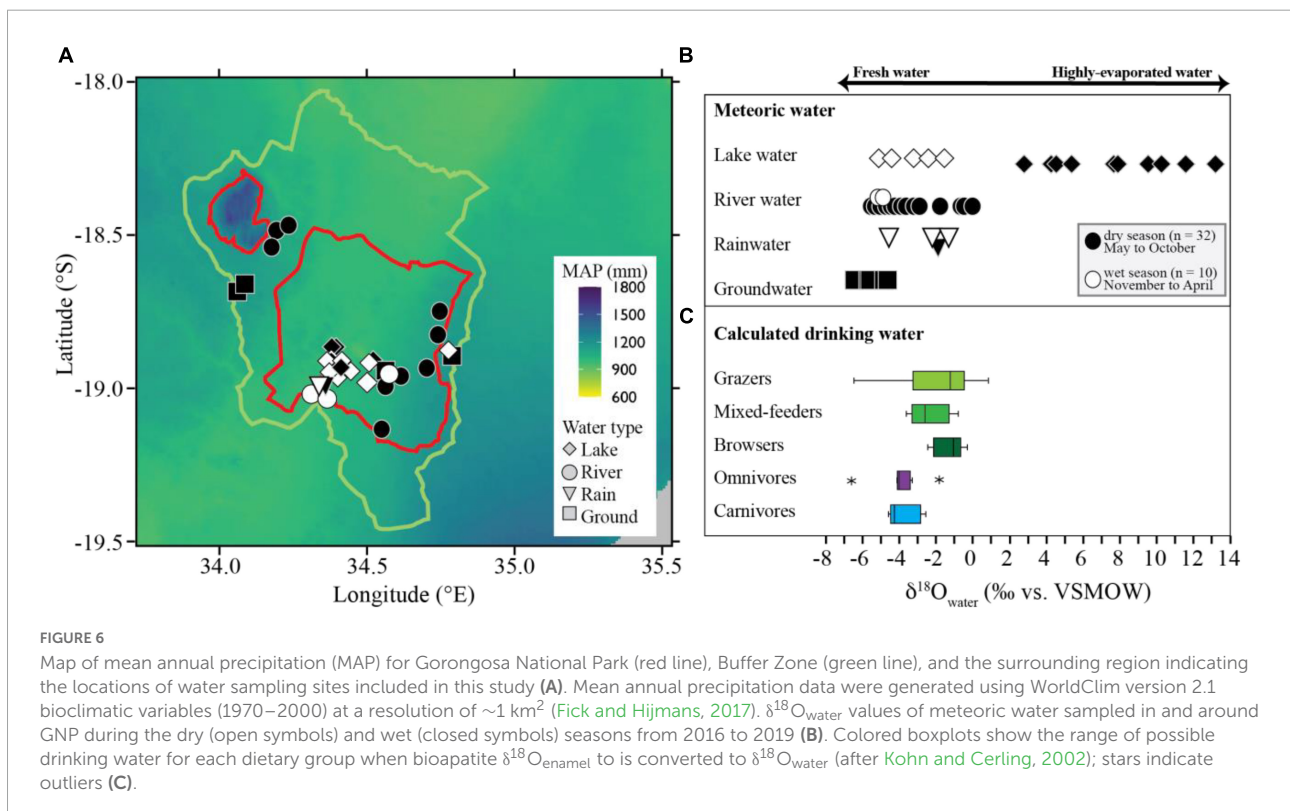
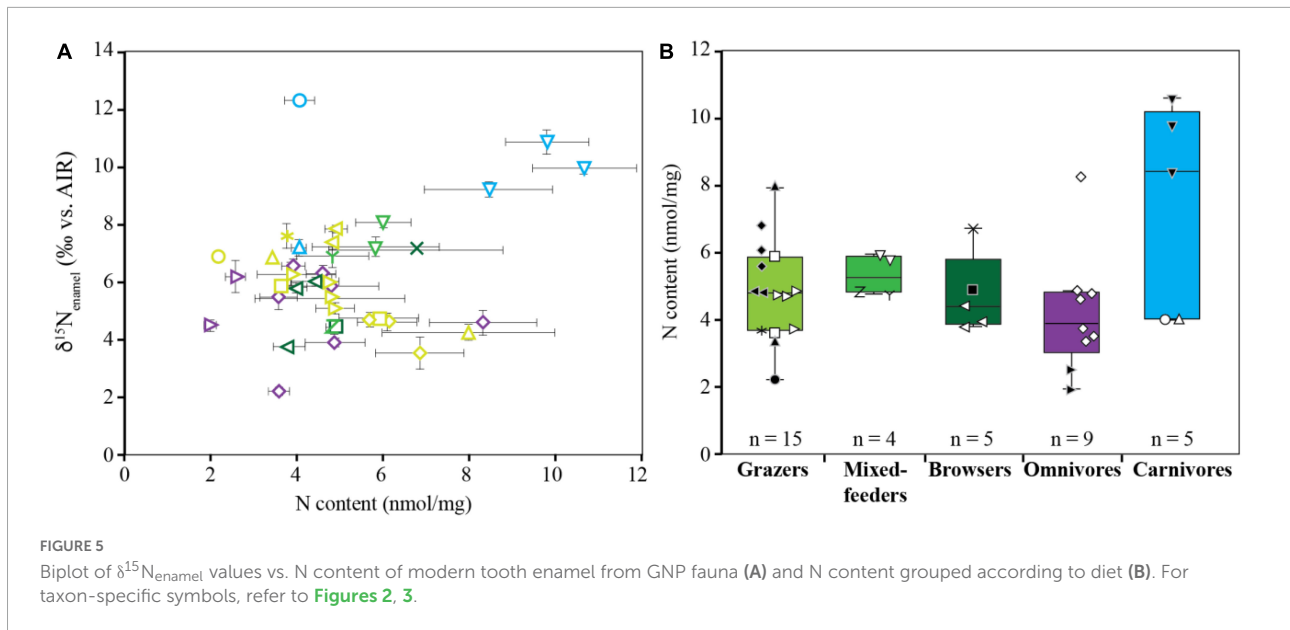
We use stable isotope values in the tooth enamel of modern fauna living in and around GNP to (a) understand food web dynamics and dietary behavior in this well-constrained faunal community, (b) provide the first test of the suitability of using $\delta^{15}\text{N}_{\text{enamel}}$ data in a natural ecosystem to reconstruct trophic level, (c) apply a new method for measuring $\delta^{13}\text{C}_{\text{enamel}}$ and $\delta^{18}\text{O}_{\text{enamel}}$ of $\leq 100 \mu\text{g}$ of tooth enamel, and (d) investigate isotopic niche overlap, size, and separation within and between groups by analyzing the three isotope systems ($\delta^{13}\text{C}_{\text{enamel}}$, $\delta^{15}\text{N}_{\text{enamel}}$, and $\delta^{18}\text{O}_{\text{enamel}}$).

Reconstructing trophic levels using $\delta^{15}\text{N}_{\text{enamel}}$

Gorongosa carnivores have an average of 4.0‰ higher $\delta^{15}\text{N}_{\text{enamel}}$ values and occupy distinct isotopic niche space compared to herbivores (Figures 3, 7). This trophic enrichment agrees well with a documented 3–5‰ increase in $\delta^{15}\text{N}$ between diet and consumer reported by numerous large-scale ecological studies using other biological tissues (e.g., Schoeninger and DeNiro, 1984; Bocherens and Drucker, 2003; Caut et al., 2009). These results clearly show that $\delta^{15}\text{N}_{\text{enamel}}$ values obtained with the “oxidation-denitrification method” reflect expected patterns in natural settings and have great potential for reconstructing (paleo)food webs.

Herbivore $\delta^{15}\text{N}_{\text{enamel}}$

In our dataset, herbivore $\delta^{15}\text{N}_{\text{enamel}}$ values vary by 4.3‰, with values ranging from 3.8 to 8.1‰ (Figure 3A). Similar variability has been reported for herbivores in studies using bone collagen and is believed to be related to differences in feeding strategies (e.g., grazing vs. browsing), digestive physiology (e.g., ruminant vs. non-ruminant), the nutritional value of the consumed plant material (e.g., low vs. high protein content), foraging habitat (e.g., savanna vs. forest) (Ambrose, 1991; Robbins et al., 2005), and location (Leichtler et al., 2022). However, we do not observe any significant differences in $\delta^{15}\text{N}_{\text{enamel}}$ between herbivores grouped according to grazing,



browsing, or mixed-feeding (Figure 3A), ruminant vs. non-ruminant, or water dependency (Figure 4A).

These results suggest that local variation in plant $\delta^{15}\text{N}$ values (likely associated with variation in soil $\delta^{15}\text{N}$) appears to be the principal mechanism influencing herbivore $\delta^{15}\text{N}$ values. The observed 4.3‰ variation in $\delta^{15}\text{N}_{\text{enamel}}$ within the herbivore trophic level agrees well with the reported 4‰ baseline variation

in $\delta^{15}\text{N}$ of savanna plants from different microhabitats of Kruger National Park in South Africa (Codron et al., 2005). This dry savanna biome lies ca. 650 km southwest of GNP and is similar in size to GNP and its Buffer Zone. In Kruger, some deciduous trees (e.g., *Cassia abbreviate*) and tussock-forming grasses (e.g., *Heteropogon contortus* and *Themeda triandra*) have low $\delta^{15}\text{N}$ values ($\leq 1.5\text{‰}$), while other trees (e.g., *Ficus*

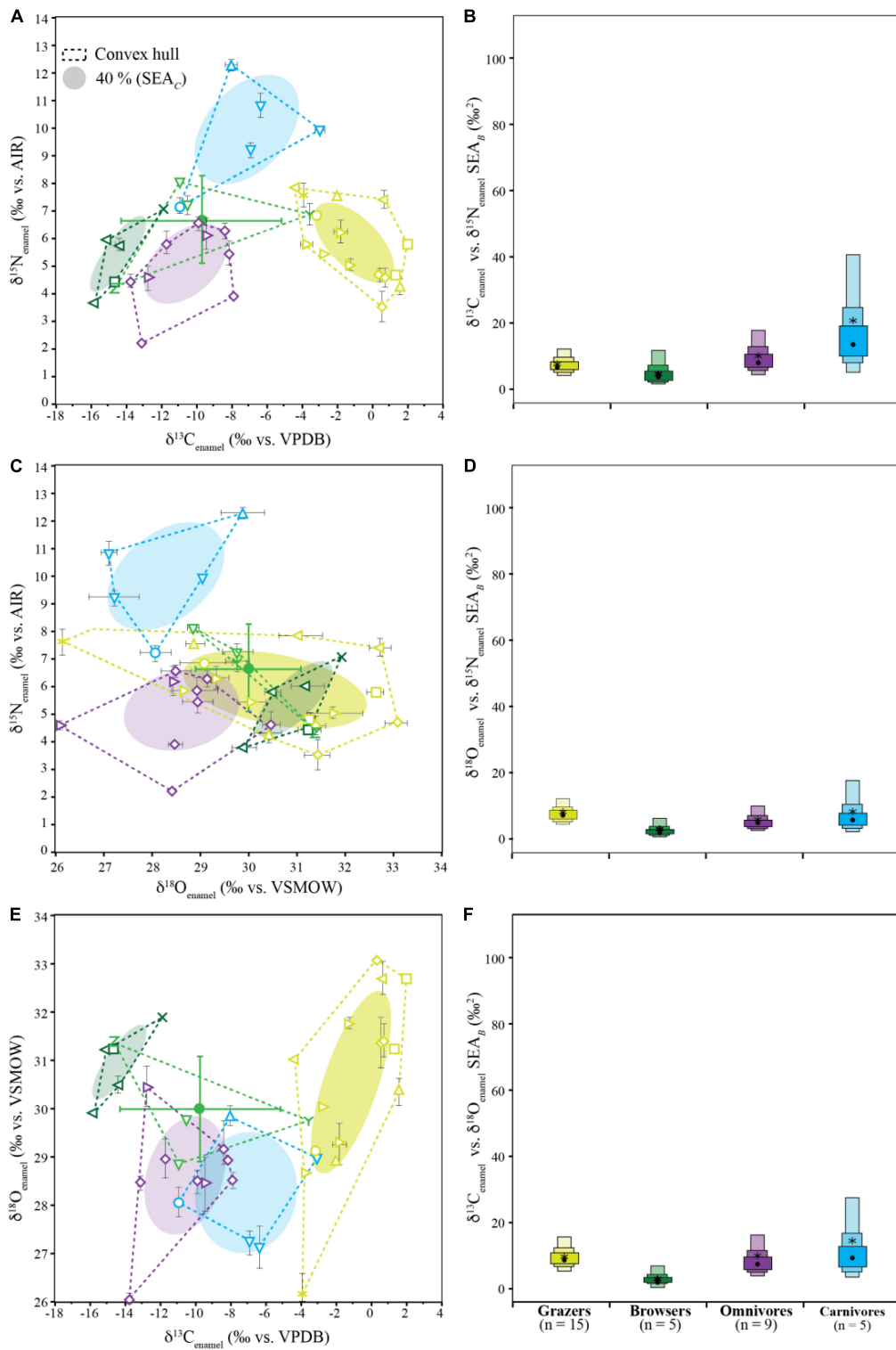


FIGURE 7

Biplots (A,C,E) and calculated SEA_B boxplots (B,D,F) for $\delta^{13}\text{C}_{\text{enamel}}$ vs. $\delta^{15}\text{N}_{\text{enamel}}$ (A,B), $\delta^{18}\text{O}_{\text{enamel}}$ vs. $\delta^{15}\text{N}_{\text{enamel}}$ (C,D), and $\delta^{13}\text{C}_{\text{enamel}}$ vs. $\delta^{18}\text{O}_{\text{enamel}}$ (E,F). Biplots show raw isotope values with 1σ standard deviation, convex hulls encompass the full variation in the data, and ellipses indicate 40% estimated SEA_C for Gorongosa fauna grouped by diet (light green: grazers; bright green: mixed-feeders; dark green: browsers; purple: omnivores; blue: carnivores; for taxon-specific symbols refer to Figure 2). Boxplots show the variability of SEA_B , with 50, 75, and 95% credible intervals represented by light, medium, and dark colored boxes, respectively. Black dots are the SEA_B mode and stars are the calculated SEA_C , which correspond to biplot ellipses. Box plots and SEA_C of mixed-feeders are not shown due to their small sample size ($n = 4$) instead, their mean values and 1σ standard deviation are given (green cycle with error bar).

sycomorus, *Grewia* sp., and *Ziziphus mucronate*) and grasses (e.g., *Dactyloctenium australe*) have much higher $\delta^{15}\text{N}$ values ($>5.0\%$). All these plant taxa are present in GNP and, therefore, available as a food resource for the studied herbivores. Different ungulate individuals occupy different habitats within GNP (e.g., floodplain vs. savanna), where they are observed to eat radically different diets (Becker et al., 2021), and therefore possibly consume plants with varying nitrogen isotope values.

Therefore, the large variety of herbivore $\delta^{15}\text{N}_{\text{enamel}}$ is expected and probably reflects variations in plant $\delta^{15}\text{N}$ values in GNP with its diverse microhabitats, soil types, plant taxa, and water availability, even if faunal migration ranges are relatively small (Stalmans and Beilfuss, 2008).

Omnivore $\delta^{15}\text{N}_{\text{enamel}}$

The $\delta^{15}\text{N}_{\text{enamel}}$ values for omnivores are significantly different from those of carnivores, but not herbivores (Figure 3A and Table 1). Our omnivore dataset includes seven baboons (*Papio ursinus* with genetic variants of *P. cynocephalus*, Santander et al., 2022) and two bushpigs (*Potamochoerus larvatus*); the two taxa are indistinguishable in their $\delta^{15}\text{N}_{\text{enamel}}$ values.

Plant material consumed by baboons mainly consists of specific plant parts such as fruits, drupes, tubers, and other underground materials, depending on the habitat and foraging season (Nowak, 1999). The baboons sampled for this study have $\delta^{15}\text{N}_{\text{enamel}}$ values between 2.2 and 6.6‰, a large range of variation in $\delta^{15}\text{N}_{\text{enamel}}$ despite the fact that six of the seven specimens were collected within a small geographic area (0.6 km²) of open C₄ grasslands with some isolated acacia trees and could possibly have even belonged to the same troop (Figure 2 and Supplementary Table 2). This large intra-taxon variation indicates a diverse and flexible diet and possibly distinct individual dietary preferences.

Baboons and bushpigs are omnivorous generalists, their diet often consisting of up to 30% of animal resources (e.g., insects, small mammals, small reptiles, eggs, and nestlings). GNP baboons have been observed to consume mussels and snails, as well as to hunt small mammals (e.g., warthog, reedbuck or bushbuck infants, and ducklings) on rare occasions, usually during the birthing season (L. Lewis-Bevan, personal communication). However, only adults (usually dominant males) have been directly observed consuming meat, although high-ranking adult females occasionally consume scraps discarded by the males. Young, low-ranking troop members, however, whose teeth are still mineralizing, rarely have access to these protein-rich resources before vultures claim leftovers. The teeth sampled for this study would have formed during this juvenile period, which likely explains the low $\delta^{15}\text{N}_{\text{enamel}}$ values observed for the GNP baboons. Moreover, while occasional meat consumption should increase omnivore $\delta^{15}\text{N}_{\text{enamel}}$ values, available data on bone collagen and fecal samples show that chacma baboons tend to have low $\delta^{15}\text{N}$ values

compared to sympatric herbivores (Ambrose and DeNiro, 1986; Codron et al., 2006). This pattern is possibly related to the consumption of N₂-fixing plants, underground storage organs, fruits, roots, and termites, all of which have relatively low $\delta^{15}\text{N}$ values (Codron et al., 2005, 2007).

Despite the fact that the two sampled bushpigs (*Potamochoerus larvatus*) were found over 120 km apart, they have similar $\delta^{15}\text{N}_{\text{enamel}}$ values, which are comparable to those of the baboons (Figure 3A). While baboons are not observed to scavenge, bushpigs do eat carrion, and their opportunistic diet includes roots, crops, bulbs, insects, and fallen fruit (e.g., discarded by baboons; Ghiglieri et al., 2008).

Carnivore $\delta^{15}\text{N}_{\text{enamel}}$

Carnivore $\delta^{15}\text{N}_{\text{enamel}}$ values are significantly higher than the values of the other dietary groups ($p < 0.001$; Figure 3A). Compared to their potential prey the GNP carnivores had, on average 4.0‰ higher $\delta^{15}\text{N}_{\text{enamel}}$ values. This trophic enrichment falls well within the expected range of 3–5‰ between trophic levels (Figure 1). While our carnivore dataset is small, niche separation between carnivore taxa is observed. The lion (*Panthera leo*) has the highest $\delta^{15}\text{N}_{\text{enamel}}$ value (12.3‰) recorded in the GNP dataset, indicating that it fed on prey with high $\delta^{15}\text{N}_{\text{enamel}}$ values. In contrast, the only other felid, a single leopard (*Panthera pardus*), has the lowest $\delta^{15}\text{N}_{\text{enamel}}$ value of all the carnivores and is the only individual that overlaps with herbivores (but not omnivores). Its $\delta^{15}\text{N}_{\text{enamel}}$ value of 7.2‰ is several permil lower than the other analyzed carnivores. $\delta^{15}\text{N}_{\text{enamel}}$ values lower than coexisting carnivores have also been reported from two leopards from Angola (Leichtler et al., 2022). This is probably the result of different habitat use and prey preference, which is also apparent in the leopard's more negative $\delta^{13}\text{C}_{\text{enamel}}$ values compared to the GNP lion and crocodiles (refer to $\delta^{13}\text{C}_{\text{enamel}}$ section; Figure 3B). Accordingly, our bulk $\delta^{15}\text{N}_{\text{enamel}}$ data possibly reflect a time in the animal's life where it fed on prey with low $\delta^{15}\text{N}$ tissue values.

Only one apex predator, the Nile crocodile (*Crocodylus niloticus*), sustains a stable population in GNP (Stalmans et al., 2014). In this study, only fully grown *C. niloticus* were sampled, as physiological and ontogenetic factors such as body size can influence their $\delta^{15}\text{N}$ values (Villamarin et al., 2018). GNP crocodiles are reported to be highly generalized predators, feeding on carnivorous and herbivorous fish species (i.e., Siluriformes) as well as mammalian prey (Wilson, 2014). However, crocodylians which consume a large variety of prey from tropical coastal floodplains derive the majority of their nutrition from the consumption of (occasional) terrestrial prey (Adame et al., 2018). Thus, while the aquatic prey consumed by GNP crocodiles may influence the $\delta^{15}\text{N}$ values of the crocodiles to some degree (these resources derive from the aquatic food chain with a possibly different N isotope baseline), the nitrogen isotope values of the crocodylians should reflect mostly their terrestrial prey. The GNP crocodylian's $\delta^{15}\text{N}_{\text{enamel}}$ values fall well

between those of the two felids, suggesting that both groups share isotopic niche space.

We analyzed all carnivore specimens available from GNP at the time of this study. The lion died naturally within the park's boundaries (Figure 1) and the leopard was poached within the Buffer Zone (the body was later confiscated by park rangers, exact coordinates were not reported). Planned analyses will incorporate additional GNP predators as well as aquatic resources for their isotopic composition once they become available, to fully understand the observed patterns. However, even our small dataset shows promising results from an ecological perspective, and more importantly, shows expected $\delta^{15}\text{N}$ patterns in enamel.

Nitrogen contents in tooth enamel

Nitrogen contents of mammalian tooth enamel from GNP fauna have a relatively small range (2.0–8.3 nmol/mg) and do not show any correlation with $\delta^{15}\text{N}_{\text{enamel}}$. Moreover, N contents are remarkably similar across different individuals and dietary groups ($p = 0.357$) and are in good agreement with those previously reported for rodents in a controlled feeding experiment (Leichliter et al., 2021) and other mammals from different sites across Africa (Leichliter et al., 2022). These findings suggest that mammalian tooth enamel N content is relatively consistent regardless of feeding strategy.

Interestingly, the nitrogen content of crocodile tooth enamel is, on average, nearly 5 nmol/mg higher than any of the mammalian taxa [9.6 ± 1.1 nmol/mg for crocodiles ($n = 3$) vs. 4.7 ± 1.4 nmol/mg for mammals ($n = 35$); Figure 5 and Table 1]. While the structure of reptilian enamel is reported to be generally similar to mammalian enamel (Dauphin and Williams, 2008), we were unable to find any information regarding the N content of reptilian tooth enamel. Our results suggest that reptilian tooth enamel contains more nitrogen than mammalian tooth enamel, possibly as the result of differences in their respective physiology or mineralization mechanisms. We considered the possibility that the higher N content of the reptilian specimens was caused by contamination with dentin during sampling. Measurements of dentin N content of in-house standard AG-Lox ($n = 3$) indicate that the nitrogen content is substantially lower in dentin than in enamel after the reductive-oxidative cleaning (Supplementary Table 9). This is not surprising because dentin has a lower proportion of mineral-bound organic material that can survive the cleaning treatment. Therefore, possible contamination with dentin cannot be the cause of the elevated N contents of the analyzed crocodile enamel.

Overall, the fact that mammalian tooth enamel N content is relatively consistent and is not correlated with $\delta^{15}\text{N}_{\text{enamel}}$ suggests that N content could be used in paleodietary studies as a diagnostic tool to assess potential signs of diagenetic alteration or

contamination by exogenous organic N, as it has been suggested for invertebrate organisms, such as foraminifera and corals (Ren et al., 2009; Straub et al., 2013; Martinez-Garcia et al., 2014; Ren et al., 2017; Wang et al., 2017; Kast et al., 2019; Auderset et al., 2022).

Reconstructing plant-based diet using $\delta^{13}\text{C}_{\text{enamel}}$

Our $\delta^{13}\text{C}_{\text{enamel}}$ data reflects the niche partitioning that is present between taxa feeding on different plants, and animals consuming prey with different feeding strategies (Figures 3B, 7).

Herbivore $\delta^{13}\text{C}_{\text{enamel}}$

Herbivore $\delta^{13}\text{C}_{\text{enamel}}$ data from GNP indicate a wide range of foraging strategies, including mixed-feeders, browsers, and grazers (Figure 3B), reflecting the wide range of ecosystems present in the park (Figure 2).

Within the GNP herbivores, browsers have $\delta^{13}\text{C}_{\text{enamel}}$ values of -11.8‰ to -15.8‰ , reflecting diets consisting almost exclusively of C_3 plants ($\geq 93\%$; calculated after Cerling et al., 2011). Most grazers, in contrast, have $\delta^{13}\text{C}_{\text{enamel}}$ values $> -2\text{‰}$ which reflect at least 70% of C_4 consumption. Three individuals are hypergrazers with $> 95\%$ C_4 grass consumption (one buffalo and two sable antelopes). However, five individuals (two warthogs and one zebra, waterbuck, and hippo) that are typically considered to be grazing species have somewhat low $\delta^{13}\text{C}_{\text{enamel}}$ value (-2.7‰ to -4.3‰), reflecting up to 45% of C_3 intake (refer to Figure 3B). This unusually high C_3 consumption may be the result of grazing on C_3 grasses (*Oryza longistaminata*), which grow in the floodplain grasslands near Lake Urema, or feeding on forbs and other C_3 understory vegetation. For example, hippos are reported to feed on *Oryza* (Noirard et al., 2008), and we observed warthogs in GNP digging up the underground rhizomes of *Oryza* and sedges.

Mixed-feeders usually have a diet of $> 30\%$ C_4 grass and $> 30\%$ C_3 browse, resulting in $\delta^{13}\text{C}_{\text{enamel}}$ values between -2‰ and -8‰ . In the GNP dataset, only the impala (*Aepyceros melampus*) has a mixed-feeder $\delta^{13}\text{C}_{\text{enamel}}$ value (Figure 3B). Impalas are known to exhibit dietary flexibility and rely on browse in some areas and graze in others, sometimes on a seasonal basis which can result in a large range of $\delta^{13}\text{C}_{\text{enamel}}$ values (Monro, 1980; Sponheimer et al., 2003). The single impala specimen from GNP has a $\delta^{13}\text{C}_{\text{enamel}}$ value of -3.6‰ corresponding to ca. 37% C_3 consumption. In contrast, the analyzed nyala (*Tragelaphus angasii*) and the two elephants (*Loxodonta africana*) primarily browsed ($\geq 85\%$ C_3 biomass). African elephants are also mixed-feeding generalists, but with a diet that consists largely of C_3 browse (Codron et al., 2012), agreeing well with our data. Gorongosa elephants have been regularly observed raiding nutritious crops (e.g., fruits, maize,

and tubers) in the Buffer Zone when the quality and abundance of natural forages are low within the park (Branco et al., 2019b). The majority of these crops are C₃ plants (e.g., banana, tomato, papaya, peas, sweet potato, pumpkin, and sorghum; Sage and Zhu, 2011); only maize and sugar cane are C₄. Hence, crop raiding probably contributed to the low $\delta^{13}\text{C}_{\text{enamel}}$ values observed for the elephants.

Herbivore $\delta^{13}\text{C}_{\text{enamel}}$ values do not differ when grouped by digestive physiology (Figure 4B), as ruminants include bovids with diverse feeding behaviors (grazers, mixed-feeders, and browsers) and have a large range in $\delta^{13}\text{C}_{\text{enamel}}$ values which overlap with the non-ruminants. In our dataset, the non-ruminants are mostly grazers with high $\delta^{13}\text{C}_{\text{enamel}}$ values, but also include elephants that ate C₃ plants. Obligate drinkers have statistically higher $\delta^{13}\text{C}_{\text{enamel}}$ values compared to non-obligate drinkers, likely reflecting the higher water content of browse compared to graze (i.e., mostly C₄ grasses) which must be supplemented with drinking water.

Overall, $\delta^{13}\text{C}_{\text{enamel}}$ data reflects the diversity of GNP habitats, providing niches for herbivores with different feeding behaviors, ranging from hyperbrowsers to hypergrazers.

Omnivore $\delta^{13}\text{C}_{\text{enamel}}$

Omnivore $\delta^{13}\text{C}_{\text{enamel}}$ values (−13.7 to −8.2‰) indicate a predominantly C₃ diet for Gorongosa baboons and bushpigs (Figure 3B). Grasses and other C₄-based foods comprise less than a third of the bulk diet of all sampled individuals, and three individuals (two primates and one suid) consumed an exclusively C₃ diet (Figure 3C and Supplementary Table 1). One of the bushpigs, which are typically forest-dwelling, was collected in a C₄-dominated grassland (*Digitaria swaziensis*; Supplementary Table 1), yet its low $\delta^{13}\text{C}_{\text{enamel}}$ value (−13.7‰) reflects pure browsing, suggesting that dietary preference rather than the locally dominant vegetation drove the feeding behavior in this individual. Overall, our findings are consistent with previously published $\delta^{13}\text{C}$ data for baboons and bushpigs which also indicate a diet consisting largely of C₃ foods (e.g., Ambrose and DeNiro, 1986; Thackeray et al., 1996; Codron et al., 2006; Venter and Kalule-Sabiti, 2016 and references therein).

Carnivore $\delta^{13}\text{C}_{\text{enamel}}$

Few studies have investigated the $\delta^{13}\text{C}$ (or $\delta^{18}\text{O}$) ecology of carnivores in Africa (Codron et al., 2007, 2016, 2018; Voigt et al., 2018; Hopley et al., 2022), which makes interpretation of the GNP dataset challenging. The GNP carnivores have $\delta^{13}\text{C}_{\text{enamel}}$ values which fall between those of herbivores and omnivores, indicating that grazers, browsers, mixed-feeders, and/or omnivores were all potentially consumed (Figure 3B). The three crocodiles have the highest $\delta^{13}\text{C}_{\text{enamel}}$ values (between −6.9‰ and −3.1‰), which could be the result of the consumption of aquatic resources, or grazers and mixed-feeders, while the single leopard individual's low $\delta^{13}\text{C}_{\text{enamel}}$ value (−11.0‰) indicates that it was feeding almost exclusively

on browsing taxa. The lion's higher $\delta^{13}\text{C}_{\text{enamel}}$ (−8.1‰) indicates that this individual preyed on more grazers compared to the leopard. According to field observations (Bouley et al., 2018), waterbuck ($\delta^{13}\text{C}_{\text{enamel}} = -4.3$ to 0.6‰) make up ca. 60% of the prey biomass consumed by Gorongosa's lions. The lion's intermediate $\delta^{13}\text{C}_{\text{enamel}}$ value indicates that it must have also consumed some prey with lower $\delta^{13}\text{C}$ values such as browsers (e.g., kudu, eland, and bushbuck) or mixed-feeders with a C₃-dominated diet (e.g., nyala). The specimen for this study was collected in the tall-grass margins that border the savanna woodlands, which is a preferred hunting habitat for lions as it provides access to abundant grazing, browsing, and mixed-feeding prey. The lion's $\delta^{13}\text{C}_{\text{enamel}}$ is nearly 3‰ higher than that of the leopard, indicating that it focused more on grazing prey while the leopard consumed more browsers. A similar difference in $\delta^{13}\text{C}_{\text{enamel}}$ between leopard and lion is observed in a modern felid dataset from Turkana Basin (Kenya; Hopley et al., 2022).

Reconstructing drinking behavior using $\delta^{18}\text{O}_{\text{enamel}}$ and $\delta^{18}\text{O}_{\text{water}}$

$\delta^{18}\text{O}_{\text{water}}$ of meteoric water sampled between 2016 and 2019 within GNP agree well with data reported from meteoric water stations of the Global Network of Isotopes (GNI) in Precipitation (sampled in Chitengo in 2010 to 2011; IAEA/WISER, 2020a) and GNI in Rivers (Pungwe River in 2009; IAEA/WISER, 2020b). Moreover, data fall on the Local Meteoric Water Line (LMWL) and Local Evaporation Line (LEL) established with $\delta^{18}\text{O}_{\text{water}}$ and deuterium ($\delta^2\text{H}_{\text{water}}$) data of samples from springs, boreholes, river, and Lake Urema taken in the Urema catchment in the period 2006–2010 (Steinbruch and Weise, 2014). Note that the $\delta^2\text{H}_{\text{water}}$ values are reported in Supplementary Table 2 but are not discussed in this study.

$\delta^{18}\text{O}_{\text{water}}$ of available drinking water reported in this study has a range of >20‰ (Figure 6), and varies much more than the $\delta^{18}\text{O}_{\text{enamel}}$ values measured for the fauna (i.e., ~7‰, Figure 3C). After converting bioapatite $\delta^{18}\text{O}_{\text{enamel}}$ to $\delta^{18}\text{O}_{\text{water}}$ (using equations by Kohn and Cerling, 2002), the measured range of 26.0 to 33.1‰ in $\delta^{18}\text{O}_{\text{enamel}}$ translates into the intake of water with $\delta^{18}\text{O}_{\text{water}}$ values between −6.6‰ and 1.0‰, which falls, with the exception of a hippo and a baboon specimen, in low to medium range of measured meteoric waters (−6.2 to 13.1‰; Figure 6). This indicates that the animals in this study consumed primarily fresh water that was only moderately influenced by evaporative enrichment. Time-averaging of temporal signals during the progressive mineralization of tooth enamel could dampen the variation in $\delta^{18}\text{O}_{\text{water}}$ ingested by a single individual through time (i.e., information about seasonal variability of the drinking water is lost).

Meteoric water $\delta^{18}\text{O}_{\text{water}}$

Potentially available drinking water for animals living in GNP overlaps greatly in their $\delta^{18}\text{O}_{\text{water}}$ values and falls generally between -6.2 and 0.8‰ , with the exception of dry season lake waters, which range from 2.9‰ up to 13.1‰ (Figure 6). Therefore, dry season lake water displays significantly higher $\delta^{18}\text{O}_{\text{water}}$ values, compared to all other types of water ($p < 0.001$; there is no overlap with other $\delta^{18}\text{O}_{\text{water}}$ datasets; Figure 6). During the dry season, standing water in lakes or ponds is most strongly influenced by evaporation (Clark and Fritz, 1997; Kendall and McDonnell, 1998). $\delta^{18}\text{O}_{\text{water}}$ of rainwater sampled during the wet season and rain samples were taken from the end of the dry season overlap. This agrees well with previously published isotope data from Gorongosa meteoric waters, which indicate that wet season rainfall was formed over the Indian Ocean without undergoing major fractionation, while dry season rainfall comes partly from the same source, and also indicates locally evaporated or recycled waters from the floodplains of the Urema Graben (Steinbruch and Weise, 2014).

Herbivore $\delta^{18}\text{O}_{\text{enamel}}$

With a mean of $30.6 \pm 1.6\text{‰}$ ($n = 24$) herbivores have the highest $\delta^{18}\text{O}_{\text{enamel}}$ values compared to other dietary groups (Figure 3C), but no differences are observed for browsing, mixed-feeding, or grazing taxa, indicating similar drinking behaviors, from a mix of sources, among these groups. Ranging from 26.2 to 33.1‰ , $\delta^{18}\text{O}_{\text{enamel}}$ values of grazers have the largest spread of any dietary group. In herbivores, ruminants have significantly higher $\delta^{18}\text{O}_{\text{enamel}}$ values compared to non-ruminants, but obligate drinkers do not have significantly different $\delta^{18}\text{O}_{\text{enamel}}$ values compared to non-obligate drinkers (Figure 4C). This indicates that animals had regular access to fresh water that has experienced only limited evaporation, or to leaf water and/or parts of plants that are not affected much by evaporation (e.g., stems, roots, bark, and fruits) in mesic environments.

No significant correlation was observed between $\delta^{13}\text{C}_{\text{enamel}}$ and $\delta^{18}\text{O}_{\text{enamel}}$ for most groups; however, a strong and significant positive relationship exists between $\delta^{13}\text{C}_{\text{enamel}}$ and $\delta^{18}\text{O}_{\text{enamel}}$ in grazers and obligate drinkers ($r = 0.700$; $p = 0.004$ for grazers; $r = 0.493$; $p = 0.052$ for obligate drinkers), indicating increased intake of ^{18}O -depleted water (e.g., from Lake Urema or waterholes) associated with greater C_4 plant consumption (e.g., grasses from the floodplain) for these groups.

Omnivore $\delta^{18}\text{O}_{\text{enamel}}$

Omnivore $\delta^{18}\text{O}_{\text{enamel}}$ values are significantly lower than those of herbivores but overlap with those of carnivores. The two bushpigs show slightly lower $\delta^{18}\text{O}_{\text{enamel}}$ values compared to the seven baboons. As obligate drinkers, both $\delta^{18}\text{O}_{\text{enamel}}$ values in both taxa reflect the oxygen isotope composition of local meteoric waters as expected (Moritz et al., 2012; Steinbruch and Weise, 2014). Their relatively low $\delta^{18}\text{O}_{\text{enamel}}$ values point

toward a regular recharge of their body water by drinking from meteoric sources which are only moderately influenced by evaporation (Fricke and O'Neil, 1996; Levin et al., 2006; Blumenthal et al., 2017), limited intake of evaporated plant tissues or animal fats (refer to nitrogen section; Crowley, 2012; Nelson, 2013; Carter and Bradbury, 2016), and little sweating or panting (thermoregulatory processes which induce evaporative fractionation; Kohn et al., 1996; Sponheimer and Lee-Thorp, 1999).

Carnivore $\delta^{18}\text{O}_{\text{enamel}}$

Studies about the water requirements of African savanna carnivores are rare and observations of drinking behavior in Gorongosa's felids are anecdotal; thus, oxygen stable isotope data can provide valuable additional information regarding water intake in predators.

Most African felids have low water needs and receive their moisture from the metabolic water of their prey (Bothma and Walker, 2013), but drink water from waterholes when it is available (Wilson and Mittermeier, 2009; Hayward and Hayward, 2012). Through this intake of prey body fluids and standing water, $\delta^{18}\text{O}_{\text{enamel}}$ data of lions and leopards from eastern Africa are strongly influenced by local meteoric $\delta^{18}\text{O}_{\text{water}}$, similar to what has been documented for herbivores (Kohn, 1996; Hopley et al., 2022). Gorongosa carnivores have, on average, ca. 2‰ lower $\delta^{18}\text{O}_{\text{enamel}}$ values compared to their prey (Figure 3C), and therefore relatively low calculated $\delta^{18}\text{O}_{\text{drinking-water}}$. This suggests that the GNP carnivores had access to freshwater and drank regularly. While the lion's $\delta^{18}\text{O}_{\text{enamel}}$ value overlaps with those of the herbivores, the leopard's does not, possibly indicating that the leopard consumed more fresh river water rather than evaporated lake water.

A rough linear correlation is reported between the oxygen isotopic ratios of crocodiles' phosphate tooth enamel and ambient water which is influenced by mean air temperature, diet, and physiology (Amiot et al., 2007). GNP crocodile carbonate $\delta^{18}\text{O}_{\text{enamel}}$ values are generally low, indicating that the sampled individuals lived in relatively fresh water that was rarely influenced by evaporation.

Isotopic niches and inferred ecology from paired $\delta^{13}\text{C}_{\text{enamel}}$, $\delta^{15}\text{N}_{\text{enamel}}$, and $\delta^{18}\text{O}_{\text{enamel}}$ data

Traditionally, paired carbon and nitrogen isotope values are analyzed in ecological studies to reconstruct isotopic niches and infer some trophic information (Newsome et al., 2007). Until recently, this type of reconstruction using tooth enamel has not been possible due to the methodological limitations of measuring $\delta^{15}\text{N}_{\text{enamel}}$ (Leichliter et al., 2021). This study is the first to combine nitrogen, carbon, and oxygen stable

isotope values obtained from diagenetically robust tooth enamel, permitting ecological interpretations based on the combination of these three isotopes. We compare the different pairs of isotope values ($\delta^{13}\text{C}_{\text{enamel}}-\delta^{15}\text{N}_{\text{enamel}}$, $\delta^{15}\text{N}_{\text{enamel}}-\delta^{18}\text{O}_{\text{enamel}}$, and $\delta^{13}\text{C}_{\text{enamel}}-\delta^{18}\text{O}_{\text{enamel}}$; **Figure 7**) to investigate niche overlap, size, and separation within and between dietary groups of modern fauna from GNP. Isotopic niches calculated in this way can be used to infer information about trophic ecology and resources used by determined groups (Layman et al., 2007; Newsome et al., 2007; Layman and Allgeier, 2012). Given the small sample size of the mixed-feeder ($n = 4$; not included in niche analysis), browser ($n = 5$), and carnivore ($n = 5$) groups, we consider our statistical conclusions to be preliminary but promising. Our isotopic niche results are best interpreted as (1) relative but not absolute values for niche overlap; (2) SEA_B is variable and increased sample size would likely decrease the uncertainty around the estimates and lead to a more robust analysis resolving potential size differences, but generalities are valid; and (3) unique locations in isotopic space are statistically accurate, and small changes to niche size from additional sampling would likely not move centroids enough to effect centroid distance. Additional Bayesian analyses are becoming increasingly popular in ecological studies and could also be included in future multi-isotope tooth enamel studies if sample sizes are increased. For example, 3-dimensional isotopic analysis using SIBER has proven useful for determining isotopic niches of complex trophic systems such as coral reef atolls (Cybulski et al., 2022), and other analyses such as nicheROVER allow for incorporation of additional dimensions of isotopes or other continuous ecological indicators (Swanson et al., 2015). Even with uncertainties, isotopic investigations coupled with Bayesian statistics have significant implications for future (paleo)ecological reconstructions.

In the GNP fauna, the niches of different dietary groups are completely distinct in $\delta^{13}\text{C}_{\text{enamel}}-\delta^{15}\text{N}_{\text{enamel}}$ space (**Figure 7A**), with no SEA_C overlap between any dietary groups (**Supplementary Table 6**). Thus, animals with these diets can be classified into distinct isotopic niches based on their carbon and nitrogen isotope values in our dataset. Although we cannot quantify the niche of the mixed-feeders due to limited sampling, we can explore potential overlap with other groups. For example, even with only four samples, mixed-feeders convex-hull overlaps with the omnivores niche in $\delta^{13}\text{C}_{\text{enamel}}-\delta^{15}\text{N}_{\text{enamel}}$ space. This overlap would be expected, as it occurs around typical $\delta^{13}\text{C}_{\text{enamel}}$ values for C_3 dominated diets (Cerling et al., 2003), on which GNP omnivores and some of the analyzed mixed-feeders (nyala and elephants) rely (**Figure 3B** and **Supplementary Table 1**). We would expect that even with additional sampling, isotopic niche overlap between these two groups would remain.

$\delta^{18}\text{O}$ data are not frequently used in ecological studies; however, some research has shown that $\delta^{18}\text{O}$ can complement the information provided by carbon and nitrogen (e.g.,

Crowley et al., 2015; Roberts, 2017). Gorongosa grazers exhibit a wide range of $\delta^{18}\text{O}_{\text{enamel}}$ values and share $\delta^{15}\text{N}_{\text{enamel}}-\delta^{18}\text{O}_{\text{enamel}}$ niche space with browsers (**Figures 7B,E**). Omnivores tend to have lower $\delta^{18}\text{O}_{\text{enamel}}$ values and only overlap slightly with grazers in $\delta^{15}\text{N}_{\text{enamel}}-\delta^{18}\text{O}_{\text{enamel}}$ niche space. Due to the trophic enrichment in $\delta^{15}\text{N}_{\text{enamel}}$ and relatively low $\delta^{18}\text{O}_{\text{enamel}}$ values, carnivores do not overlap with any other group in $\delta^{15}\text{N}_{\text{enamel}}-\delta^{18}\text{O}_{\text{enamel}}$ space. This shows that animals with a plant-dominated diet (i.e., herbivores and omnivores) cannot be distinguished in $\delta^{15}\text{N}_{\text{enamel}}-\delta^{18}\text{O}_{\text{enamel}}$ alone. In contrast, carnivores with their specialized diet occupy a distinct isotopic space and can be clearly distinguished from other groups, even though terrestrial mammalian and aquatic reptilian carnivores were combined in this group. While $\delta^{15}\text{N}_{\text{enamel}}$ vs. $\delta^{18}\text{O}_{\text{enamel}}$ comparisons can potentially reveal isotope niche distinction between some dietary groups, niche separation is mostly driven by trophic elevation in $\delta^{15}\text{N}_{\text{enamel}}$ in this dataset.

In $\delta^{13}\text{C}_{\text{enamel}}-\delta^{18}\text{O}_{\text{enamel}}$ space (**Figure 7C**), the SEA_C of the grazers and browsers are well separated, while omnivores and carnivores overlap by 20–30%. The convex hull of the four sampled mixed-feeders overlaps with all isotopic niches except the grazers, indicating that further sampling may lead to significant niche overlaps. In the $\delta^{13}\text{C}_{\text{enamel}}$ vs. $\delta^{18}\text{O}_{\text{enamel}}$ biplot, most of the dietary information is derived from carbon. The small trophic enrichment of 1‰ sometimes observed in $\delta^{13}\text{C}$ of tissues (DeNiro and Epstein, 1981; Schoeniger and DeNiro, 1984; Bocherens and Drucker, 2003; O'Connell et al., 2012) is obscured by differences in $\delta^{13}\text{C}$ between consumed C_3 and C_4 plants (or prey that consumed those plants; Cerling and Harris, 1999; Hopley et al., 2022), while $\delta^{18}\text{O}_{\text{enamel}}$ cannot serve as a trophic proxy (but can reveal information about drinking behavior and source waters instead). This shows that there is a minimal ecologically expected organization of isotopic niches without the information gained from $\delta^{15}\text{N}_{\text{enamel}}$ data.

In conclusion, analysis of combined carbon, nitrogen, and oxygen stable isotope values leads to the isotopic separation of grazers, browsers, omnivores, and carnivores dietary groups, with significant niche overlap of mixed-feeding herbivores with all groups expected upon further sampling. Niche separation is clearest in $\delta^{13}\text{C}_{\text{enamel}}-\delta^{15}\text{N}_{\text{enamel}}$ space with no overlap between any of the dietary groups. This illustrates the high potential of $\delta^{15}\text{N}_{\text{enamel}}$ combined with $\delta^{13}\text{C}_{\text{enamel}}$ and $\delta^{18}\text{O}_{\text{enamel}}$ measured from a single aliquot of tooth enamel for reconstructing isotopic niches and inferring dietary and trophic information. Carnivores—arguably the most isotopically distinguishable group—provide a useful example of the benefits of this type of combined isotopic approach. Typical and recent studies of trophic behavior using stable isotope data from teeth and/or bone have been limited to $\delta^{13}\text{C}$ and $\delta^{18}\text{O}$ (e.g., Domingo et al., 2020), though zinc (Bourgon et al., 2020, 2021; McCormack et al., 2021; Jaouen et al., 2022) and calcium (Martin et al., 2015, 2020, 2022) are also used for trophic studies. If we consider only $\delta^{13}\text{C}_{\text{enamel}}$ vs. $\delta^{18}\text{O}_{\text{enamel}}$, carnivores would not

occupy a distinct isotopic niche space since they would overlap with omnivores (20%) and with the mixed-feeders convex hull. Ecologically, however, carnivores occupy a distinct dietary niche, as they consume animal resources almost exclusively. In contrast, GNP omnivores (baboons and bushpigs) consume meat only occasionally while mixed-feeders rely exclusively on plant biomass. Thus, carnivores should not overlap with either group unless there is wide variation in baseline $\delta^{15}\text{N}$ (refer e.g., Schmidt and Stewart, 2003; Codron et al., 2005). The addition of $\delta^{15}\text{N}_{\text{enamel}}$ to both $\delta^{13}\text{C}_{\text{enamel}}$ and $\delta^{18}\text{O}_{\text{enamel}}$ analysis clearly shows that carnivores do occupy a statistically significant isotopic niche space, with no SEA_C overlap with any other groups' niche.

Conclusion

We present the first stable carbon, nitrogen, and oxygen isotope data from tooth enamel for fauna from GNP. We validate two novel geochemical methods and draw conclusions about the dietary patterns of animals living within this well-constrained and well-studied African ecosystem. While field observations are extremely useful for understanding the dietary ecology of modern fauna, they are very labor intensive, requiring following an individual (or a group of animals) for days or months, or the deployment and evaluation of hours of camera trap footage. Moreover, such studies often only record a snapshot in time (e.g., one single feeding event) rather than capturing long-term behavior. In contrast, our bulk stable isotope data of herbivores (including grazers, mixed-feeders, and browsers), omnivores, and carnivores, reflect $\delta^{13}\text{C}$, $\delta^{15}\text{N}$, and $\delta^{18}\text{O}$ of consumed food and water averaged over the course of tooth enamel mineralization.

Our results generally exhibit robust isotopic patterns and therefore support ecological information about the trophic level, dietary niche, and resource consumption. We show that $\delta^{15}\text{N}_{\text{enamel}}$ analyzed with the “oxidation-denitrification method” records the trophic position of an individual within its local food web. This is evidenced by a trophic enrichment of 4.0‰ between herbivores and carnivores in the GNP dataset. This method applies not only to a wide range of sample-limited ecosystems but also has potential applications in paleoecology. $\delta^{13}\text{C}_{\text{enamel}}$ analysis using the “cold trap method,” tailored to measure small sample sizes (down to 50 μg tooth enamel), distinguishes C_3 and/or C_4 biomass consumption, while $\delta^{18}\text{O}_{\text{enamel}}$ values reflect drinking water.

This first tri-isotope approach conducted on the tooth enamel of fauna from a single, well-constrained ecosystem indicates that combined C, N, and O isotope data analyses permit the separation of grazers, browsers, omnivores, and carnivores according to their isotopic niche, while preliminary analysis of mixed-feeding herbivores indicate that they cannot be clearly distinguished from other groups. This illustrates the

high potential of our multi-isotope approach for paleontological applications using diagenetically robust tooth enamel. We plan to apply this novel multi-isotope approach to recently discovered vertebrate fossils from GNP, which represent the only Miocene fossil locality in the southern East African Rift (Habermann et al., 2019; Bobe et al., 2021). Thus, the datasets presented here will serve as an excellent comparison for the interpretation of fossil stable isotope data.

Data availability statement

The original contributions presented in this study are included in the article/Supplementary material, further inquiries can be directed to the corresponding authors.

Ethics statement

Ethical review and approval was not required for the animal study because samples were taken from specimens collected after natural death and curated by the faunal bone collection of Gorongosa National Park.

Author contributions

TL and JL: conceptualization and analysis. TL, JL, AF, ND, HV, DS, and AM-G: methodology. RB and SC: Paleo-Primate Project Gorongosa direction. TL, VA, MB, DB, DRB, CC, MF, JH, FM, JM, RB, and SC: fieldwork. JM and RB: curating of PPPG collection. TL, JL, and JC: statistical analysis. TL, JL, and AM-G: writing—original draft. All authors contributed to the article and approved the submitted version.

Funding

This study was funded by the Deutsche Forschungsgemeinschaft (DFG) grant LU 2199/1-1 and Emmy Noether Fellowship LU 2199/2-1 to TL, the Max Planck Society to GH, HV, and AM-G, and the National Geographic Society grants NGS-51478R to TL and JH, NGS-57285R to SC, and NGS-51140R-18 to RB. MF worked under an FCT-funded associate researcher contract (CEECIND/01937/2017), AM-G received funding from DFG grant MA 8270/1-1, and ND from the Paul Crutzen Nobel Prize fellowship of the Max Planck Society. The Paleo-Primate-Project Gorongosa was funded by the Gorongosa Restoration Project, the Leverhulme Trust (Philip Leverhulme Prize 114 to SC); the John Fell Fund, Oxford, and the St Hugh's College, University of Oxford.

Acknowledgments

We are grateful to the Gorongosa Restoration Project and especially Greg Carr for their vital support of the Paleo-Primate Project Gorongosa. Research and export permits were granted by the Direção Nacional do Património Cultural, Mozambique, with the support of professors H. Madiquida and S. Macamo of Eduardo Mondlane University. We thank the dedicated staff from Gorongosa National Park, the *fiscals*, our students, and colleagues across many institutions who have been very enthusiastic about this project. Special thanks to P. Hammond, L. Lewis-Bevan (University of Oxford), and R. A. Farassi (Universidade Eduardo Mondlane) for first-hand observational data on Gorongosa baboons, and E. W. Negash (George Washington University) for helpful comments on the manuscript. We thank J. Delinger and M. Stalmans for their vital support and assistance with data collection throughout the years. We also thank F. Rubach, S. Brömme, M. Schmitt, B. Hinnenberg (Max Planck Institute for Chemistry, Germany), and U. Treffert (Senckenberg Biodiversity and Climate Research Centre, Frankfurt, Germany) for technical support, and I. Conti-Jerpe (UC Berkley) for the SIBER advice. This manuscript was greatly improved by the thoughtful comments of VB, JR, LK, and the editor.

References

- Abou Neel, E. A., Aljabo, A., Strange, A., Ibrahim, S., Coathup, M., Young, A. M., et al. (2016). Demineralization-rem mineralization dynamics in teeth and bone. *Int. J. Nanomed.* 11, 4743–4763. doi: 10.2147/IJN.S107624
- Adame, F., Jardine, T., Fry, B., Valdez, D., Lindner, G., Nadjji, J., et al. (2018). Estuarine crocodiles in a tropical coastal floodplain obtain nutrition from terrestrial prey. *PLoS One* 13:e0197159. doi: 10.1371/journal.pone.0197159
- Ambrose, S. H. (1986). Stable carbon and nitrogen isotope analysis of human and animal diet in Africa. *J. Hum. Evol.* 15, 707–731. doi: 10.1016/S0047-2484(86)80006-9
- Ambrose, S. H. (1991). Effects of diet, climate and physiology on nitrogen isotope abundances in terrestrial foodwebs. *J. Archaeol. Sci.* 18, 293–317. doi: 10.1016/0305-4403(91)90067-Y
- Ambrose, S. H., and DeNiro, M. J. (1986). The isotopic ecology of East-African mammals. *Oecologia* 69, 395–406. doi: 10.1007/bf00377062
- Ambrose, S. H., and Norr, L. (1993). “Experimental Evidence for the Relationship of the Carbon Isotope Ratios of Whole Diet and Dietary Protein to Those of Bone Collagen and Carbonate,” in *Prehistoric Human Bone: Archaeology at the Molecular Level*, eds J. B. Lambert and G. Grupe (Berlin: Springer Berlin Heidelberg), 1–37.
- Amiot, R., Lécuyer, C., Escarguel, G., Billon-Bruyat, J. P., Buffetaut, E., Langlois, C., et al. (2007). Oxygen isotope fractionation between crocodylian phosphate and water. *Palaeogeogr. Palaeoclimatol. Palaeoecol.* 243, 412–420. doi: 10.1016/j.palaeo.2006.08.013
- Amundson, R., Austin, A. T., Schuur, E. A. G., Yoo, K., Matzek, V., Kendall, C., et al. (2003). Global patterns of the isotopic composition of soil and plant nitrogen. *Glob. Biogeochem. Cycles* 17:31. doi: 10.1029/2002gb001903
- Arvidsson, K., Stenberg, L., Chirindja, F., Dahlin, T., Owen, R., and Steinbruch, F. (2011). A hydrogeological study of the Nhandugue River, Mozambique – A major groundwater recharge zone. *Phys. Chem. Earth* 36, 789–797. doi: 10.1016/j.pce.2011.07.036
- Atkins, J. L., Long, R. A., Pansu, J., Daskin, J. H., Potter, A. B., Stalmans, M. E., et al. (2019). Cascading impacts of large-carnivore extirpation in an African ecosystem. *Science* 364, 173–177. doi: 10.1126/science.aau3561
- Auderset, A., Moretti, S., Taphorn, B., Ebner, P. R., Kast, E., Wang, X. T., et al. (2022). Enhanced ocean oxygenation during Cenozoic warm periods. *Nature* 609, 77–82. doi: 10.1038/s41586-022-05017-0
- Ayliffe, L. K., Lister, A. M., and Chivas, A. R. (1992). The preservation of glacial-interglacial climatic signatures in the oxygen isotopes of elephant skeletal phosphate. *Palaeogeogr. Palaeoclimatol. Palaeoecol.* 99, 179–191.
- Balasse, M., Bocherens, H., and Mariotti, A. (1999). Intra-bone variability of collagen and apatite isotopic composition used as evidence of a change of diet. *J. Archaeol. Sci.* 26, 593–598.
- Becker, J. A., Hutchinson, M., Potter, A., Park, S., Guyton, J., Abernathy, K., et al. (2021). Ecological and behavioral mechanisms of density-dependent habitat expansion in a recovering African ungulate population. *Ecol. Monogr.* 91:e01476. doi: 10.1002/ECM.1476
- Behrensmeyer, A. K. (1978). Taphonomic and Ecologic Information from Bone Weathering. *Paleobiology* 4, 150–162.
- Blumenthal, S. A., Levin, N. E., Brown, F. H., Brugal, J. P., Chritz, K. L., Harris, J. M., et al. (2017). Aridity and hominin environments. *Proc. Natl. Acad. Sci. U. S. A.* 114, 7331–7336. doi: 10.1073/pnas.1700597114
- Bobe, R., Aldeias, V., Alemseged, Z., Archer, W., Aumaitre, G., Bamford, M. K., et al. (2021). The first Miocene fossils from coastal woodlands in the southern East African Rift. *Biorxiv* [Preprint]. doi: 10.1101/2021.12.16.472914
- Bobe, R., Martínez, F. I., and Carvalho, S. (2020). Primate adaptations and evolution in the Southern African Rift Valley. *Evol. Anthropol.* 29, 94–101. doi: 10.1002/evan.21826
- Bocherens, H. (2009). “Neanderthal Dietary Habits: Review of the Isotopic Evidence,” in *The Evolution of Hominin Diets: Integrating Approaches to the Study of Palaeolithic Subsistence*, eds J. J. Hublin and M. P. Richards (Dordrecht: Springer Netherlands), 241–250.

Conflict of interest

The authors declare that the research was conducted in the absence of any commercial or financial relationships that could be construed as a potential conflict of interest.

Publisher’s note

All claims expressed in this article are solely those of the authors and do not necessarily represent those of their affiliated organizations, or those of the publisher, the editors and the reviewers. Any product that may be evaluated in this article, or claim that may be made by its manufacturer, is not guaranteed or endorsed by the publisher.

Supplementary material

The Supplementary Material for this article can be found online at: <https://www.frontiersin.org/articles/10.3389/fevo.2022.958032/full#supplementary-material>

- Bocherens, H., and Drucker, D. (2003). Trophic level isotopic enrichment of carbon and nitrogen in bone collagen: Case studies from recent and ancient terrestrial ecosystems. *Int. J. Osteoarchaeol.* 13, 46–53.
- Bocherens, H., Koch, P. L., Mariotti, A., Geraads, D., and Jaeger, J. J. (1996). Isotopic biogeochemistry (^{13}C , ^{18}O) of mammalian enamel from African Pleistocene hominid sites. *Palaiois* 11, 306–318. doi: 10.2307/3515241
- Böhme, B. (2005). Geo ecology of the Lake Urema / Central Mozambique. *Freiberg Online Geosci.* 14:2005. doi: 10.23689/fdgeo-881
- Bothma, J. (2005). Water-use by southern Kalahari leopards. *S. Afr. J. Wildl. Res.* 35, 131–137. doi: 10.10520/EJC117220
- Bothma, J., and Walker, C. (2013). *Larger Carnivores of the African Savannas*. Heidelberg: Springer.
- Bouley, P., Paulo, A., Angela, M., Du Plessis, C., and Marneweck, D. G. (2021). The successful reintroduction of African wild dogs (*Lycaon pictus*) to Gorongosa National Park, Mozambique. *PLoS One* 16:e0249860. doi: 10.1371/journal.pone.0249860
- Bouley, P., Poulos, M., Branco, R., and Carter, N. H. (2018). Post-war recovery of the African lion in response to large-scale ecosystem restoration. *Biol. Conserv.* 227, 233–242. doi: 10.1016/j.biocon.2018.08.024
- Bourgon, N., Jaouen, K., Bacon, A. M., Dufour, E., McCormack, J., Tran, N. H., et al. (2021). Trophic ecology of a Late Pleistocene early modern human from tropical Southeast Asia inferred from zinc isotopes. *J. Hum. Evol.* 161:103075. doi: 10.1016/j.jhevol.2021.103075
- Bourgon, N., Jaouen, K., Bacon, A. M., Jochum, K. P., Dufour, E., Düringer, P., et al. (2020). Zinc isotopes in Late Pleistocene fossil teeth from a Southeast Asian cave setting preserve paleodietary information. *Proc. Natl. Acad. Sci. U. S. A.* 117, 4675–4681. doi: 10.1073/pnas.1911744117
- Branco, P., Merkle, J., Pringle, R., King, L., Tindall, T., Stalmans, M., et al. (2019a). An experimental test of community-based strategies for mitigating human-wildlife conflict around protected areas. *Conserv. Lett.* 13:e12679. doi: 10.1111/conl.12679
- Branco, P., Merkle, J., Pringle, R., Pansu, J., Potter, A., Reynolds, A., et al. (2019b). Determinants of elephant foraging behaviour in a coupled human-natural system: Is brown the new green?. *J. Anim. Ecol.* 88, 780–792. doi: 10.1111/1365-2656.12971
- Bryant, D. J., and Froelich, P. N. (1995). A model of oxygen isotope fractionation in body water of large mammals. *Geochim. Cosmochim. Acta* 59, 4523–4537. doi: 10.1016/0016-7037(95)00250-4
- Bryant, D. J., Koch, P. L., Froelich, P. N., Showers, W. J., and Genna, B. J. (1996). Oxygen isotope partitioning between phosphate and carbonate in mammalian apatite. *Geochim. Cosmochim. Acta* 60, 5145–5148. doi: 10.1016/S0016-7037(96)00308-0
- Cain, J. III, Owen-Smith, N., and Macandza, V. (2012). The costs of drinking: Comparative water dependency of sable antelope and zebra. *J. Zool.* 286, 58–67. doi: 10.1111/j.1469-7998.2011.00848.x
- Cantalapiedra-Hijar, G., Ortigues-Marty, I., Sepchat, B., Agabriel, J., Huneau, J. F., and Fouillet, H. (2015). Diet–animal fractionation of nitrogen stable isotopes reflects the efficiency of nitrogen assimilation in ruminants. *Br. J. Nutr.* 113, 1158–1169. doi: 10.1017/S0007114514004449
- Carter, M. L., and Bradbury, M. W. (2016). Oxygen isotope ratios in primate bone carbonate reflect amount of leaves and vertical stratification in the diet. *Am. J. Primatol.* 78, 1086–1097. doi: 10.1002/ajp.22432
- Caut, S., Angulo, E., and Courchamp, F. (2009). Variation in discrimination factors ($\Delta^{15}\text{N}$ and $\Delta^{13}\text{C}$): The effect of diet isotopic values and applications for diet reconstruction. *J. Appl. Ecol.* 46, 443–453. doi: 10.1111/j.1365-2664.2009.01620.x
- Cerling, E., Harris, J. M., and Passey, B. H. (2003). Diets of East African bovidae based on stable isotope analysis. *J. Mammal.* 84, 456–470. doi: 10.2307/1383890
- Cerling, T., Andanje, S., Blumenthal, S., Brown, F., Chritz, K., Harris, J., et al. (2015). Dietary changes of large herbivores in the Turkana Basin, Kenya from 4 to 1 Ma. *Proc. Natl. Acad. Sci. U. S. A.* 112:201513075. doi: 10.1073/pnas.1513075112
- Cerling, T. E., Bernasconi, S. M., Hofstetter, L. S., Jaggi, M., Wyss, F., Rudolf von Rohr, C., et al. (2021). CH_4/CO_2 ratios and carbon isotope enrichment between diet and breath in herbivorous mammals. *Front. Ecol. Evol.* 9:638568. doi: 10.3389/fevo.2021.638568
- Cerling, T. E., and Harris, J. M. (1999). Carbon isotope fractionation between diet and bioapatite in ungulate mammals and implications for ecological and paleoecological studies. *Oecologia* 120, 347–363. doi: 10.1007/s004420050868
- Cerling, T. E., Harris, J. M., Ambrose, S. H., Leakey, M. G., and Solounias, N. (1997). Dietary and environmental reconstruction with stable isotope analyses of herbivore tooth enamel from the Miocene locality of Fort Ternan, Kenya. *J. Hum. Evol.* 33, 635–650. doi: 10.1006/jhev.1997.0151
- Cerling, T. E., Wynn, J. G., Andanje, S. A., Bird, M. I., Korir, D. K., Levin, N. E., et al. (2011). Woody cover and hominin environments in the past 6 million years. *Nature* 476, 51–56. doi: 10.1038/nature10306
- Chinique de Armas, Y., Mavridou, A. M., Garcell Domínguez, J., Hanson, K., and Laffoon, J. (2022). Tracking breastfeeding and weaning practices in ancient populations by combining carbon, nitrogen and oxygen stable isotopes from multiple non-adult tissues. *PLoS One* 17:e0262435. doi: 10.1371/journal.pone.0262435
- Clark, I. D., and Fritz, P. (1997). *Environmental isotopes in hydrogeology*. Boca Raton: CRC press.
- Codron, D., Codron, J., Lee-Thorp, J. A., Sponheimer, M., de Ruiter, D., and Brink, J. S. (2007). Stable isotope characterization of mammalian predator–prey relationships in a South African savanna. *Eur. J. Wildl. Res.* 53, 161–170. doi: 10.1007/s10344-006-0075-x
- Codron, D., Codron, J., Sponheimer, M., and Clauss, M. (2016). Within-population isotopic niche variability in savanna mammals: Disparity between carnivores and herbivores. *Front. Ecol. Evol.* 4:15. doi: 10.3389/fevo.2016.0015
- Codron, D., Lee-Thorp, J. A., Sponheimer, M., de Ruiter, D., and Codron, J. (2006). Inter- and intrahabitat dietary variability of chacma baboons (*Papio ursinus*) in South African savannas based on fecal $\delta^{13}\text{C}$, $\delta^{15}\text{N}$, and $\delta^2\text{H}$. *Am. J. Phys. Anthropol.* 129, 204–214. doi: 10.1002/ajpa.20253
- Codron, D., Radloff, F. G., Codron, J., Kerley, G. I., and Tambling, C. J. (2018). Meso-carnivore niche expansion in response to an apex predator's reintroduction—a stable isotope approach. *Afr. J. Wildl. Res.* 48, 1–16. doi: 10.3957/056.048.013004
- Codron, J., Codron, D., Lee-Thorp, J. A., Sponheimer, M., Bond, W. J., de Ruiter, D., et al. (2005). Taxonomic, anatomical, and spatio-temporal variations in the stable carbon and nitrogen isotopic compositions of plants from an African savanna. *J. Archaeol. Sci.* 32, 1757–1772. doi: 10.1016/j.jas.2005.06.006
- Codron, J., Codron, D., Sponheimer, M., Kirkman, K., Duffy, K. J., Raubenheimer, E. J., et al. (2012). Stable isotope series from elephant ivory reveal lifetime histories of a true dietary generalist. *Proc. R. Soc. B Biol. Sci.* 279, 2433–2441. doi: 10.1098/rspb.2011.2472
- Coplen, T. B. (1988). Normalization of oxygen and hydrogen isotope data. *Chem. Geol.* 72, 293–297. doi: 10.1016/0168-9622(88)90042-5
- Correia, M., Timóteo, S., Rodriguez-Echeverria, S., Mazars-Simon, A., and Heleno, R. (2017). Refaunation and the reinstatement of the seed-dispersal function in Gorongosa National Park. *Conserv. Biol.* 31, 76–85. doi: 10.1111/cobi.12782
- Crowley, B. (2012). Stable Isotope Techniques and Applications for Primatologists. *Int. J. Primatol.* 33, 673–701. doi: 10.1007/s10764-012-9582-7
- Crowley, B. E., Melin, A. D., Yeakel, J. D., and Dominy, N. J. (2015). Do oxygen isotope values in collagen reflect the ecology and physiology of neotropical mammals?. *Front. Ecol. Evol.* 3:127. doi: 10.3389/fevo.2015.00127
- Cumming, D., Mackie, C., Magane, S., and Taylor, R. (1994). *Aerial census of large herbivores in the Gorongosa National Park and the Marromeu Area of the Zambezi Delta in Mozambique: June 1994*. Harare, ZW: IUCN ROSA.
- Cybulski, J. D., Skinner, C., Wan, Z., Wong, C. K. M., Toonen, R. J., Gaither, M. R., et al. (2022). Improving stable isotope assessments of inter- and intra-species variation in coral reef fish trophic strategies. *Ecol. Evol.* 12:e9221. doi: 10.1002/ece3.9221
- Dag, O., Dolgun, A., and Konar, N. M. (2018). onewaytests: An R Package for One-Way Tests in Independent Groups Designs. *R J.* 10, 175–199.
- Dailey-Chwalibóg, T., Huneau, J. F., Mathé, V., Kolsteren, P., Mariotti, F., Mostak, M. R., et al. (2020). Weaning and stunting affect nitrogen and carbon stable isotope natural abundances in the hair of young children. *Sci. Rep.* 10:2522. doi: 10.1038/s41598-020-59402-8
- Daskin, J. H., Stalmans, M., and Pringle, R. M. (2016). Ecological legacies of civil war: 35-year increase in savanna tree cover following wholesale large-mammal declines. *J. Ecol.* 104, 79–89. doi: 10.1111/1365-2745.12483
- Dauphin, Y., and Williams, C. (2008). Chemical composition of enamel and dentine in modern reptile teeth. *Mineral. Mag.* 72, 247–250. doi: 10.1180/minmag.2008.072.1.247

- DeNiro, M. J., and Epstein, S. (1981). Influence of diet on the distribution of nitrogen isotopes in animals. *Geochim. Cosmochim. Acta* 45, 341–351. doi: 10.1016/0016-7037(81)90244-1
- Domingo, L., Tomassini, R. L., Montalvo, C. I., Sanz-Pérez, D., and Alberdi, M. T. (2020). The Great American Biotic Interchange revisited: A new perspective from the stable isotope record of Argentine Pampas fossil mammals. *Sci. Rep.* 10:1608. doi: 10.1038/s41598-020-58575-6
- Dunham, K. M. (2004). *Aerial Survey of Large Herbivores in Gorongosa National Park, Mozambique: 2004*. Cambridge MA: The Gregory C. Carr Foundation.
- Dutton, P., and Carvalho, F. (2002). Final Report for the GERFFA Project on the Status of Fauna in the Sofala Province 1990–2001, with Reference to Previous Data. Unpublished consultancy report. Maputo, Mozambique.
- Easter, T., Bouley, P., and Carter, N. (2019). Opportunities for biodiversity conservation outside of Gorongosa National Park, Mozambique: A multispecies approach. *Biol. Conserv.* 232, 217–227. doi: 10.1016/j.biocon.2019.02.007
- Evans, R. D. (2001). Physiological mechanisms influencing plant nitrogen isotope composition. *Trends Plant Sci.* 6, 121–126. doi: 10.1016/S1360-1385(01)01889-1
- Fick, S. E., and Hijmans, R. J. (2017). WorldClim 2: New 1-km spatial resolution climate surfaces for global land areas. *Int. J. Climatol.* 37, 4302–4315. doi: 10.1002/joc.5086
- Fox-Dobbs, K., Bump, J. K., Peterson, R. O., Fox, D. L., and Koch, P. (2007). Carnivore-specific stable isotope variables and variation in the foraging ecology of modern and ancient wolf populations: Case studies from Isle Royale, Minnesota, and La Brea. *Can. J. Zool.* 85, 458–471. doi: 10.1139/Z07-018
- Fricke, H. C., and O'Neil, J. R. (1996). Inter- and intra-tooth variation in the oxygen isotope composition of mammalian tooth enamel phosphate: Implications for palaeoclimatological and palaeobiological research. *Palaeogeogr. Palaeoclimatol. Palaeoecol.* 126, 91–99. doi: 10.1016/S0031-0182(96)00072-7
- Fuller, B. T., Fuller, J. L., Harris, D. A., and Hedges, R. E. M. (2006). Detection of breastfeeding and weaning in modern human infants with carbon and nitrogen stable isotope ratios. *Am. J. Phys. Anthropol.* 129, 279–293. doi: 10.1002/ajpa.20249
- Fulton, J., Arthur, M., Thomas, R., and Freeman, K. (2018). Pigment carbon and nitrogen isotopic signatures in euxinic basins. *Geobiology* 16, 429–445. doi: 10.1111/gbi.12285
- Gaynor, K., Branco, P., Long, R., Gonçalves, D., Granli, P., and Poole, J. (2018). Effects of human settlement and roads on diel activity patterns of elephants (*Loxodonta africana*). *Afr. J. Ecol.* 56, 872–881. doi: 10.1111/aje.12552
- Gaynor, K. M., Daskin, J. H., Rich, L. N., and Brashares, J. S. (2021). Postwar wildlife recovery in an African savanna: Evaluating patterns and drivers of species occupancy and richness. *Anim. Conserv.* 24, 510–511. doi: 10.1111/acv.12661
- Ghiglieri, M., Butynski, T., Struhsaker, T., Leland, L., Wallis, S., and Waser, P. (2008). Bush pig (*Potamochoerus porcus*) polychromatism and ecology in Kibale Forest, Uganda. *Afr. J. Ecol.* 20, 231–236. doi: 10.1111/j.1365-2028.1982.tb00298.x
- Gil-Bona, A., and Bidlack, F. B. (2020). Tooth enamel and its dynamic protein matrix. *Int. J. Mol. Sci.* 21:4458. doi: 10.3390/ijms21124458
- Goldberg, M., Kulkarni, A. B., Young, M., and Boskey, A. (2011). Dentin: Structure, composition and mineralization. *Front. Biosci.* 3:711–735. doi: 10.2741/e281
- Guyton, J. A., Pansu, J., Hutchinson, M. C., Kartzinel, T. R., Potter, A. B., Coverdale, T. C., et al. (2020). Trophic rewinding revives biotic resistance to shrub invasion. *Nat. Ecol. Evol.* 4, 712–724. doi: 10.1038/s41559-019-1068-y
- Habermann, J. M., Alberti, M., Aldeias, V., Alemseged, Z., Archer, W., Bamford, M., et al. (2019). Gorongosa by the sea: First Miocene fossil sites from the Urema Rift, central Mozambique, and their coastal paleoenvironmental and paleoecological contexts. *Palaeogeogr. Palaeoclimatol. Palaeoecol.* 514, 723–738. doi: 10.1016/j.palaeo.2018.09.032
- Hamilton, W. J. III (1986). Namib desert chacma baboon (*Papio ursinus*) use of food and water resources during a food shortage. *Madoqua* 1986, 397–407. doi: 10.10520/AJA10115498_477
- Hammer, Ø., Harper, D. A., and Ryan, P. D. (2001). PAST: Paleontological statistics software package for education and data analysis. *Palaeontol. Electron.* 4, 1–9.
- Hammond, P., Lewis-Bevan, L., Biro, D., and Carvalho, S. (2022). Risk perception and terrestriality in primates: A quasi-experiment through habituation of chacma baboons (*Papio ursinus*) in Gorongosa National Park, Mozambique. *Am. J. Biol. Anthropol.* 179, 48–59. doi: 10.1002/ajpa.24567
- Hartman, G. (2010). Are elevated $\delta^{15}\text{N}$ values in herbivores in hot and arid environments caused by diet or animal physiology?. *Funct. Ecol.* 25, 122–131. doi: 10.1111/j.1365-2435.2010.01782.x
- Hayward, M. W., and Hayward, M. D. (2012). Waterhole use by African Fauna. *S. Afr. J. Wildl. Res.* 42, 117–127.
- Hempson, G. P., Archibald, S., and Bond, W. J. (2015). A continent-wide assessment of the form and intensity of large mammal herbivory in Africa. *Science* 350, 1056–1061. doi: 10.1126/science.aac7978
- Hopley, P. J., Cerling, T. E., Crété, L., Werdelin, L., Mwebi, O., Manthi, F. K., et al. (2022). Stable isotope analysis of carnivores from the Turkana Basin, Kenya: Evidence for temporally-mixed fossil assemblages. *Quat. Int.* doi: 10.1016/j.quaint.2022.04.004
- Hoppe, K. A. (2006). Correlation between the oxygen isotope ratio of North American bison teeth and local waters: Implication for paleoclimatic reconstructions. *Earth Planet. Sci. Lett.* 244, 408–417. doi: 10.1016/j.epsl.2006.01.062
- Iacumin, P., Bocherens, H., Mariotti, A., and Longinelli, A. (1996). Oxygen isotope analyses of co-existing carbonate and phosphate in biogenic apatite: A way to monitor diagenetic alteration of bone phosphate?. *Earth Planet. Sci. Lett.* 142, 1–6. doi: 10.1016/0012-821X(96)00093-3
- IAEA/WISER (2020a). *Global Network of Isotopes in Precipitation*. Available online at: <https://www.iaea.org/services/networks/gnip> (accessed on Mar 11, 2022).
- IAEA/WISER (2020b). *Global Network of Isotopes in Rivers*. Available online at: <https://www.iaea.org/services/networks/gnir> (accessed on Mar 11, 2022).
- Jackson, A., Inger, R., Parnell, A., and Bearhop, S. (2011). Comparing isotopic niche width among and within communities: SIBER – Stable Isotope Bayesian Ellipses in R. *J. Anim. Ecol.* 80, 595–602. doi: 10.1111/j.1365-2656.2011.01806.x
- Jaouen, K., Villalba-Mouco, V., Smith, G. M., Trost, M., Leichter, J., Lüdecke, T., et al. (2022). A Neandertal dietary conundrum: New insights provided by tooth enamel Zn isotopes from Gabasa, Spain. *Proc. Natl. Acad. Sci. U. S. A.* 119:e2109315119. doi: 10.1073/pnas.2109315119
- Kassambra, A. (2021). *rstatix: Pipe-friendly framework for basic statistical tests. R package version 0.7.0*. Available online at: <https://CRAN.R-project.org/package=rstatix> (accessed September 29, 2022).
- Kast, E. R., Griffiths, M. L., Kim, S. L., Rao, Z. C., Shimada, K., Becker, M. A., et al. (2022). Cenozoic megatooth sharks occupied extremely high trophic positions. *Sci. Adv.* 8:eabl6529. doi: 10.1126/sciadv.abl6529
- Kast, E. R., Stolper, D. A., Auderset, A., Higgins, J. A., Ren, H., Wang, X. T., et al. (2019). Nitrogen isotope evidence for expanded ocean suboxia in the early Cenozoic. *Science* 364, 386–389. doi: 10.1126/science.aau5784
- Kendall, C., and McDonnell, J. J. (1998). *Isotope tracers in catchment hydrology*. Amsterdam: Elsevier.
- Kingston, J. D., and Harrison, T. (2007). Isotopic dietary reconstructions of Pliocene herbivores at Laetoli: Implications for early hominin paleoecology. *Palaeogeogr. Palaeoclimatol. Palaeoecol.* 243, 272–306. doi: 10.1016/j.palaeo.2006.08.002
- Knapp, A., Sigman, D., and Lipschultz, F. (2005). N isotopic composition of dissolved organic nitrogen and nitrate at the Bermuda Atlantic time-series study site. *Glob. Biogeochem. Cycles* 19. doi: 10.1029/2004GB002320
- Koch, P. L. (2007). “Isotopic Study of the Biology of Modern and Fossil Vertebrates,” in *Stable Isotopes in Ecology and Environmental Science*, eds R. Michener and K. Lajtha (Hoboken, NJ: Wiley), 99–154.
- Koch, P. L., Tuross, N., and Fogel, M. L. (1997). The effects of sample treatment and diagenesis on the isotopic integrity of carbonate in biogenic hydroxylapatite. *J. Archaeol. Sci.* 24, 417–429. doi: 10.1006/jasc.1996.0126
- Kohn, M. J. (1996). Predicting animal $\delta^{18}\text{O}$: Accounting for diet and physiological adaptation. *Geochim. Cosmochim. Acta* 60, 4811–4829. doi: 10.1016/S0016-7037(96)00240-2
- Kohn, M. J. (2010). Carbon isotope compositions of terrestrial C3 plants as indicators of (paleo)ecology and (paleo)climate. *Proc. Natl. Acad. Sci. U. S. A.* 107:19691. doi: 10.1073/pnas.1004933107
- Kohn, M. J., and Cerling, T. E. (2002). “Stable Isotope Compositions of Biological Apatite,” in *Phosphates. Geochemical, Geobiological, and Materials Importance*, eds M. J. Kohn, J. Rakovan, and J. M. Hughes (Washington, DC: Mineralogical Society of America), 455–488.

- Kohn, M. J., Schoeninger, M. J., and Valley, J. W. (1996). Herbivore tooth oxygen isotope compositions: Effects of diet and physiology. *Geochim. Cosmochim. Acta* 60, 3889–3896. doi: 10.1016/0016-7037(96)00248-7
- Krajcarz, M. T., Krajcarz, M., and Bocherens, H. (2018). Collagen-to-collagen prey-predator isotopic enrichment ($\Delta^{13}\text{C}$, $\Delta^{15}\text{N}$) in terrestrial mammals - a case study of a subfossil red fox den. *Palaeogeogr. Palaeoclimatol. Palaeoecol.* 490, 563–570. doi: 10.1016/j.palaeo.2017.11.044
- Lacruz, R. S., Habelitz, S., Wright, J. T., and Paine, M. L. (2017). Dental enamel formation and implications for oral health and disease. *Physiol. Rev.* 97, 939–993. doi: 10.1152/physrev.00030.2016
- Layman, C., and Allgeier, J. (2012). Characterizing trophic ecology of generalist consumers: A case study of the invasive lionfish in The Bahamas. *Mar. Ecol. Progress Ser.* 448, 131–141. doi: 10.3354/meps09511
- Layman, C. A., Arrington, D. A., Montaña, C. G., and Post, D. M. (2007). Can stable isotope ratios provide for community-wide measures of trophic structure?. *Ecology* 88, 42–48. doi: 10.1890/0012-9658(2007)88[42:csirpf]2.0.co;2
- Lee-Thorp, J., and Van der Merwe, N. J. (1987). Carbon isotope analysis of fossil bone apatite. *S. Afr. J. Sci.* 83, 712–715.
- Leichliter, J. N., Lüdecke, T., Foreman, A., Bourgon, N., Vonhof, H., Soukavaty, V., et al. (2022). Nitrogen isotopic composition of tooth enamel organic matter records trophic position in modern and fossil ecosystems. *Res. Square* [Preprint]. doi: 10.21203/rs.3.rs-1942250/v1
- Leichliter, J. N., Lüdecke, T., Foreman, A. D., Duprey, N. N., Winkler, D. E., Kast, E. R., et al. (2021). Nitrogen isotopes in tooth enamel record diet and trophic level enrichment: Results from a controlled feeding experiment. *Chem. Geol.* 563:120047. doi: 10.1016/j.chemgeo.2020.120047
- Levin, N. E., Cerling, T. E., Passey, B. H., Harris, J. M., and Ehleringer, J. R. (2006). A stable isotope aridity index for terrestrial environments. *Proc. Natl. Acad. Sci. U. S. A.* 103, 11201–11205. doi: 10.1073/pnas.0604719103
- Lüdecke, T., Kullmer, O., Wacker, U., Sandrock, O., Fiebig, J., Schrenk, F., et al. (2018). Dietary versatility of Early Pleistocene hominins. *Proc. Natl. Acad. Sci. U. S. A.* 115, 13330–13335. doi: 10.1073/pnas.1809439115
- Lüdecke, T., Mulch, A., Kullmer, O., Sandrock, O., Thiemeyer, H., Fiebig, J., et al. (2016). Stable isotope dietary reconstructions of herbivore enamel reveal heterogeneous wooded savanna ecosystems in the Plio-Pleistocene Malawi Rift. *Palaeogeogr. Palaeoclimatol. Palaeoecol.* 459, 170–181. doi: 10.1016/j.palaeo.2016.07.010
- Lueders-Dumont, J. A., Wang, X. T., Jensen, O. P., Sigman, D. M., and Ward, B. B. (2018). Nitrogen isotopic analysis of carbonate-bound organic matter in modern and fossil fish otoliths. *Geochim. Cosmochim. Acta* 224, 200–222. doi: 10.1016/j.gca.2018.01.001
- Lüttge, U. (2004). Ecophysiology of Crassulacean Acid Metabolism (CAM). *Ann. Bot.* 93, 629–652. doi: 10.1093/aob/mch087
- Ma, Y., Weldeab, S., Schneider, R. R., Andersen, N., Garbe-Schönberg, D., and Friedrich, T. (2021). Strong Southern African Monsoon and weak Mozambique Channel throughflow during Heinrich events: Implication for Agulhas leakage. *Earth Planet. Sci. Lett.* 574:117148. doi: 10.1016/j.epsl.2021.117148
- Martin, J. E., Hassler, A., Montagnac, G., Therrien, F., and Balter, V. (2022). The stability of dinosaur communities before the K-Pg boundary: A perspective from southern Alberta using calcium isotopes as a dietary proxy. *GSA Bull.* 134, 2548–2560. doi: 10.1130/b36222.1
- Martin, J. E., Tacaal, T., Adnet, S., Girard, C., and Balter, V. (2015). Calcium isotopes reveal the trophic position of extant and fossil elasmobranchs. *Chem. Geol.* 415, 118–125. doi: 10.1016/j.chemgeo.2015.09.011
- Martin, J. E., Tacaal, T., Braga, J., Cerling, T. E., and Balter, V. (2020). Calcium isotopic ecology of Turkana Basin hominins. *Nat. Commun.* 11:3587. doi: 10.1038/s41467-020-17427-7
- Martinez, F. I., Capelli, C., Ferreira da Silva, M. J., Aldeias, V., Alemseged, Z., Archer, W., et al. (2019). A missing piece of the Papio puzzle: Gorongosa baboon phenostructure and intrageneric relationships. *J. Hum. Evol.* 130, 1–20. doi: 10.1016/j.jhevol.2019.01.007
- Martinez-Garcia, A., Jung, J., Ai, X. E., Sigman, D. M., Auderset, A., Duprey, N. N., et al. (2022). Laboratory Assessment of the Impact of Chemical Oxidation, Mineral Dissolution, and Heating on the Nitrogen Isotopic Composition of Fossil-bound Organic Matter. *Geochem. Geophys. Geosyst.* 23:e2022GC010396. doi: 10.1029/2022GC010396
- Martinez-Garcia, A., Sigman, D. M., Ren, H., Anderson, R. F., Straub, M., Hoderl, D. A., et al. (2014). Iron Fertilization of the Subantarctic Ocean During the Last Ice Age. *Science* 343, 1347–1350.
- McCormack, J., Szpak, P., Bourgon, N., Richards, M., Hyland, C., Méjean, P., et al. (2021). Zinc isotopes from archaeological bones provide reliable trophic level information for marine mammals. *Commun. Biol.* 4:683. doi: 10.1038/s42003-021-02212-z
- Merceron, G., Berlioz, E., Vonhof, H., Green, D., Garel, M., and Tütken, T. (2021). Tooth tales told by dental diet proxies: An alpine community of sympatric ruminants as a model to decipher the ecology of fossil fauna. *Palaeogeogr. Palaeoclimatol. Palaeoecol.* 562:110077. doi: 10.1016/j.palaeo.2020.110077
- Monro, R. H. (1980). Observations on the Feeding Ecology of Impala. *S. Afr. J. Zool.* 15, 107–110. doi: 10.1080/02541858.1980.11447695
- Moritz, G. L., Fourie, N., Yeakel, J. D., Phillips-Conroy, J. E., Jolly, C. J., Koch, P. L., et al. (2012). Baboons, Water, and the Ecology of Oxygen Stable Isotopes in an Arid Hybrid Zone. *Physiol. Biochem. Zool.* 85, 421–430. doi: 10.1086/667533
- Muschinski, J., Biro, D., Lewis-Bevan, L., and Carvalho, S. (2019). Could it be culture? An inter-troop comparison of baboon behaviour in Gorongosa National Park, Mozambique. *Neuroscience* 91, 350–351.
- Nelson, S. (2013). Chimpanzee fauna isotopes provide new interpretations of fossil ape and hominin ecologies. *Proc. Biol. Sci. R. Soc.* 280:20132324. doi: 10.1098/rspb.2013.2324
- Newsome, S., Rio, C., Bearhop, S., and Phillips, D. (2007). A niche for isotopic ecology. *Front. Ecol. Environ.* 5:429–436. doi: 10.1890/060150.1
- Nicholson, M. J. (1985). The water requirements of livestock in Africa. *Outl. Agric.* 14, 156–164. doi: 10.1177/003072708501400401
- Noirard, C., Le Berre, M., Ramousse, R., and Lena, J. P. (2008). Seasonal variation of thermoregulatory behaviour in the *Hippopotamus (Hippopotamus amphibius)*. *J. Ethol.* 26, 191–193. doi: 10.1007/s10164-007-0052-1
- Nowak, R. M. (1999). *Walker's mammals of the world*. Baltimore, MD: Johns Hopkins University Press.
- O'Connell, T. C., Kneale, C. J., Tasevska, N., and Kuhnle, G. G. C. (2012). The diet-body offset in human nitrogen isotopic values: A controlled dietary study. *Am. J. Phys. Anthropol.* 149, 426–434. doi: 10.1002/ajpa.22140
- Pansu, J., Guyton, J. A., Potter, A. B., Atkins, J. L., Daskin, J. H., Wursten, B., et al. (2019). Trophic ecology of large herbivores in a reassembling African ecosystem. *J. Ecol.* 107, 1355–1376. doi: 10.1111/1365-2745.13113
- Passey, B. H., and Cerling, T. E. (2002). Tooth enamel mineralization in ungulates: Implications for recovering a primary isotopic time-series. *Geochim. Cosmochim. Acta* 66, 3225–3234. doi: 10.1016/S0016-7037(02)00933-X
- Pearcy, R. W., and Ehleringer, J. (1984). Comparative ecophysiology of C3 and C4 plants. *Plant Cell Environ.* 7, 1–13. doi: 10.1111/j.1365-3040.1984.tb01194.x
- Pederzani, S., and Britton, K. (2019). Oxygen isotopes in bioarchaeology: Principles and applications, challenges and opportunities. *Earth Sci. Rev.* 188, 77–107. doi: 10.1016/j.earscirev.2018.11.005
- Pinzone, M., Damseaux, F., Michel, L. N., and Das, K. (2019). Stable isotope ratios of carbon, nitrogen and sulphur and mercury concentrations as descriptors of trophic ecology and contamination sources of Mediterranean whales. *Chemosphere* 237:124448. doi: 10.1016/j.chemosphere.2019.124448
- Polissar, P. J., Fulton, J. M., Junium, C. K., Turich, C. C., and Freeman, K. H. (2009). Measurement of ^{13}C and ^{15}N Isotopic Composition on Nanomolar Quantities of C and N. *Anal. Chem.* 81, 755–763. doi: 10.1021/ac801370c
- Pringle, R. M. (2017). Upgrading protected areas to conserve wild biodiversity. *Nature* 546, 91–99. doi: 10.1038/nature22902
- R Core Team (2022). *R: A language and environment for statistical computing*. Vienna: R Foundation for Statistical Computing.
- Ren, H., Sigman, D. M., Martínez-García, A., Anderson, R. F., Chen, M. T., and Ravelo, A. C. (2017). Impact of glacial/interglacial sea level change on the ocean nitrogen cycle. *Proc. Natl. Acad. Sci. U. S. A.* 114, E6759–E6766. doi: 10.1073/pnas.1701315114
- Ren, H., Sigman, D. M., Meckler, A. N., Plessen, B., Robinson, R. S., Rosenthal, Y., et al. (2009). Foraminiferal Isotope Evidence of Reduced Nitrogen Fixation in the Ice Age Atlantic Ocean. *Science* 323, 244–248. doi: 10.1126/science.1165787
- Robbins, C. T., Felicetti, L. A., and Sponheimer, M. (2005). The effect of dietary protein quality on nitrogen isotope discrimination in mammals and birds. *Oecologia* 144, 534–540. doi: 10.1007/s00442-005-0021-8
- Roberts, P. (2017). Stable carbon, oxygen, and nitrogen, isotope analysis of plants from a South Asian tropical forest: Implications for primatology. *Am. J. Primatol.* 79. doi: 10.1002/ajp.22656

- Robinson, D. (2001). $\delta^{15}\text{N}$ as an integrator of the nitrogen cycle. *Trends Ecol. Evol.* 16, 153–162. doi: 10.1016/S0169-5347(00)02098-X
- Robinson, R. S., Brunelle, B. G., and Sigman, D. M. (2004). Revisiting nutrient utilization in the glacial Antarctic: Evidence from a new method for diatom-bound N isotopic analysis. *Paleoceanography* 19:A3001. doi: 10.1029/2003pa000996
- Sage, R. F., and Zhu, X.-G. (2011). Exploiting the engine of C_4 photosynthesis. *J. Exp. Bot.* 62, 2989–3000. doi: 10.1093/jxb/err179
- Sakae, T., Suzuki, K., and Kozawa, Y. (1997). “A short review of studies on chemical and physical properties of enamel crystallites,” in *Tooth Enamel Microstructure: Proceedings of the enamel microstructure workshop*, (Boca Raton, FL: CRC Press).
- Santander, C., Molinaro, L., Mutti, G., Martínez, F. I., Mathe, J., Ferreira da Silva, M. J., et al. (2022). Genomic variation in baboons from central Mozambique unveils complex evolutionary relationships with other *Papio* species. *BMC Ecol. Evol.* 22:44. doi: 10.1186/s12862-022-01999-7
- Schemmel, F., Mikes, T., Rojaj, B., and Mulch, A. (2013). The impact of topography on isotopes in precipitation across the Central Anatolian Plateau (Turkey). *Am. J. Sci.* 313, 61–80. doi: 10.2475/02.2013.01
- Schmidt, S., and Stewart, G. R. (2003). $\delta^{15}\text{N}$ values of tropical savanna and monsoon forest species reflect root specialisations and soil nitrogen status. *Oecologia* 134, 569–577. doi: 10.1007/s00442-002-1150-y
- Schoeniger, M. J., and DeNiro, M. J. (1984). $^{15}\text{N}/^{14}\text{N}$ ratios of bone collagen reflect marine and terrestrial components of prehistoric diets. *Geochim. Cosmochim. Acta* 48, 625–639. doi: 10.1126/science.6344217
- Schoeniger, M. J., and DeNiro, M. J. (1984). Nitrogen and carbon isotopic composition of bone collagen from marine and terrestrial animals. *Geochim. Cosmochim. Acta* 48, 625–639. doi: 10.1016/0016-7037(84)90091-7
- Sealy, J. C., van der Merwe, N. J., Thorp, J. A. L., and Lanham, J. L. (1987). Nitrogen isotopic ecology in southern Africa: Implications for environmental and dietary tracing. *Geochim. Cosmochim. Acta* 51, 2707–2717. doi: 10.1016/0016-7037(87)90151-7
- Segalen, L., Lee-Thorp, J. A., and Cerling, T. (2007). Timing of C_4 grass expansion across sub-Saharan Africa. *J. Hum. Evol.* 53, 549–559. doi: 10.1016/j.jhevol.2006.12.010
- Sigman, D. M., Casciotti, K. L., Andreani, M., Barford, C., Galanter, M., and Böhlke, J. K. (2001). A bacterial method for the nitrogen isotopic analysis of nitrate in seawater and freshwater. *Anal. Chem.* 73, 4145–4153.
- Smith, B. N., and Epstein, S. (1971). Two categories of c/c ratios for higher plants. *Plant Physiol.* 47, 380–384. doi: 10.1104/pp.47.3.380
- Sponheimer, M., Grant, R., Ruiters, D., Lee-Thorp, J., Codron, D., and Codron, J. (2003). Diets of impala from Kruger National Park: Evidence from stable carbon isotopes. *Koedoe* 46, 101–106. doi: 10.4102/koedoe.v46i1.43
- Sponheimer, M., and Lee-Thorp, J. A. (1999). Oxygen Isotopes in Enamel Carbonate and their Ecological Significance. *J. Archaeol. Sci.* 26, 723–728. doi: 10.1006/jasc.1998.0388
- Stalmans, M. (2012). *Monitoring the recovery of wildlife in the Parque Nacional da Gorongosa through aerial surveys. A preliminary analysis*. Sofala: Parque Nacional da Gorongosa.
- Stalmans, M., and Beilfuss, R. (2008). *Landscapes of the gorongosa national park*. Available online at: https://www.researchgate.net/publication/314878798_Landscapes_of_the_Gorongosa_National_Park
- Stalmans, M., Peel, M., and Massad, T. (2014). *Aerial Wildlife Count of the Parque Nacional Da Gorongosa, Mozambique, October 2014*. Sofala: Parque Nacional da Gorongosa.
- Stalmans, M. E., Massad, T. J., Peel, M. J. S., Tarnita, C. E., and Pringle, R. M. (2019). War-induced collapse and asymmetric recovery of large-mammal populations in Gorongosa National Park, Mozambique. *PLoS One* 14:e0212864. doi: 10.1371/journal.pone.0212864
- Stanton, K., and Carlson, S. (2004). Microscale $\delta^{18}\text{O}$ and $\delta^{13}\text{C}$ isotopic analysis of an ontogenetic series of the hadrosaurid dinosaur *Edmontosaurus*: Implications for physiology and ecology. *Palaeogeogr. Palaeoclimatol. Palaeoecol.* 206, 257–287. doi: 10.1016/j.palaeo.2004.01.007
- Steinbruch, F. (2010). Geology and geomorphology of the Urema Graben with emphasis on the evolution of Lake Urema. *J. Afr. Earth Sci.* 58, 272–284. doi: 10.1016/j.jafrearsci.2010.03.007
- Steinbruch, F., and Merkel, B. (2008). Characterization of a Pleistocene thermal spring in Mozambique. *Hydrogeol. J.* 16, 1655–1668. doi: 10.1007/s10040-008-0343-9
- Steinbruch, F., and Weise, S. (2014). Analysis of Water Stable Isotopes fingerprinting to inform conservation management : Lake Urema Wetland System, Mozambique. *Phys. Chem. Earth* 72–75, 13–23. doi: 10.1016/j.pce.2014.09.007
- Steinhour, W. D., Stokes, M. R., Clark, J. H., Rogers, J. A., Davis, C. L., and Nelson, D. R. (1982). Estimation of the proportion of non-ammonia-nitrogen reaching the lower gut of the ruminant derived from bacterial and protozoal nitrogen. *Br. J. Nutr.* 48, 417–431. doi: 10.1079/BJN19820124
- Straub, M., Sigman, D. M., Ren, H., Martínez-García, A., Meckler, A. N., Hain, M. P., et al. (2013). Changes in North Atlantic nitrogen fixation controlled by ocean circulation. *Nature* 501, 200–203. doi: 10.1038/nature12397
- Sutoh, M., Koyama, T., and Yoneyama, T. (1987). Variations of natural ^{15}N abundances in the tissues and digesta of domestic animals. *Radioisotopes* 36, 74–77. doi: 10.3769/radioisotopes.36.2_74
- Swanson, H. K., Lysy, M., Power, M., Stasko, A. D., Johnson, J. D., and Reist, J. D. (2015). A new probabilistic method for quantifying n-dimensional ecological niches and niche overlap. *Ecology* 96, 318–324. doi: 10.1890/14-0235.1
- Syväranta, J., Lensu, A., Marjomäki, T. J., Oksanen, S., and Jones, R. I. (2013). An Empirical Evaluation of the Utility of Convex Hull and Standard Ellipse Areas for Assessing Population Niche Widths from Stable Isotope Data. *PLoS One* 8:e56094. doi: 10.1371/journal.pone.0056094
- Tejada-Lara, J. V., MacFadden, B. J., Bermudez, L., Rojas, G., Salas-Gismondí, R., and Flynn, J. J. (2018). Body mass predicts isotope enrichment in herbivorous mammals. *Proc. R. Soc. B Biol. Sci.* 285:20181020. doi: 10.1098/rspb.2018.1020
- Teruel, J. D. D., Alcolea, A., Hernández, A., and Ruiz, A. J. O. (2015). Comparison of chemical composition of enamel and dentine in human, bovine, porcine and ovine teeth. *Arch. Oral Biol.* 60, 768–775. doi: 10.1016/j.archoralbio.2015.01.014
- Thackeray, J. F., Henzi, S. P., and Brain, C. (1996). Stable carbon and nitrogen isotope analysis of bone collagen in *Papio cynocephalus ursinus*: Comparison with ungulates and *Homo sapiens* from southern and East African environments. *S. Afr. J. Sci.* 92, 209–213.
- Tinley, K. L. (1977). *Framework of the Gorongosa ecosystem*. Pretoria: University of Pretoria.
- Tsutaya, T., and Yoneda, M. (2015). Reconstruction of breastfeeding and weaning practices using stable isotope and trace element analyses: A review. *Am. J. Phys. Anthropol.* 156, 2–21. doi: 10.1002/ajpa.22657
- Turner, T. F., Collyer, M. L., and Krabbenhoft, T. J. (2010). A general hypothesis-testing framework for stable isotope ratios in ecological studies. *Ecology* 91, 2227–2233. doi: 10.1890/09-1454.1
- Ungar, P. S. (2010). *Mammal Teeth: Origin, Evolution, and Diversity*. Baltimore, MD: Johns Hopkins University Press.
- Uno, K. T., Rivals, F., Bibi, F., Pante, M., Njau, J., and de la Torre, I. (2018). Large mammal diets and paleoecology across the Oldowan–Acheulean transition at Olduvai Gorge, Tanzania from stable isotope and tooth wear analyses. *J. Hum. Evol.* 120, 76–91. doi: 10.1016/j.jhevol.2018.01.002
- Venter, J., and Kalule-Sabiti, M. (2016). Diet Composition of the Large Herbivores in Mkambati Nature Reserve, Eastern Cape, South Africa. *Afr. J. Wildl. Res.* 46, 49–56. doi: 10.3957/056.046.0049
- Villamarin, F., Jardine, T. D., Bun, S. E., Marioni, B., and Magnusson, W. E. (2018). Body size is more important than diet in determining stable-isotope estimates of trophic position in crocodylians. *Sci. Rep.* 8:2020. doi: 10.1038/s41598-018-19918-6
- Voigt, C. C., Krolf, M., Menges, V., Wachter, B., and Melzheimer, J. (2018). Sex-specific dietary specialization in a terrestrial apex predator, the leopard, revealed by stable isotope analysis. *J. Zool.* 306, 1–7. doi: 10.1111/jzo.12566
- Vonhof, H., De Graaf, S., Spero, H., Schiebel, R., Verdegaaal, S., Metcalfe, B., et al. (2020a). High-precision stable isotope analysis of $<5\ \mu\text{g}\ \text{CaCO}_3$ samples by continuous-flow mass spectrometry. *Rapid Commun. Mass Spectrom.* 34:e8878. doi: 10.1002/rcm.8878
- Vonhof, H., Tütken, T., Leichter, J. N., Lüdecke, T., and Haug, G. H. (2020b). “High-precision stable isotope analysis of structural carbonate in $<100\ \mu\text{g}$ tooth enamel samples by continuous-flow mass spectrometry,” in *The Society of Vertebrate Paleontology 80th Annual Meeting*. Available online at: https://vertpaleo.org/wp-content/uploads/2021/03/SVP_2020_Program-Abstracts-Volume-FINAL-for-Publishing-1.27.2021.pdf
- Wang, X. T., Prokopenko, M. G., Sigman, D. M., Adkins, J. F., Robinson, L. F., Ren, H., et al. (2014). Isotopic composition of carbonate-bound organic nitrogen

in deep-sea scleractinian corals: A new window into past biogeochemical change. *Earth Planet. Sci. Lett.* 400, 243–250.

Wang, X. T., Sigman, D. M., Cohen, A. L., Sinclair, D. J., Sherrell, R. M., Weigand, M. A., et al. (2015). Isotopic composition of skeleton-bound organic nitrogen in reef-building symbiotic corals: A new method and proxy evaluation at Bermuda. *Geochim. Cosmochim. Acta* 148, 179–190.

Wang, X. T., Sigman, D. M., Prokopenko, M. G., Adkins, J. F., Robinson, L. F., Hines, S. K., et al. (2017). Deep-sea coral evidence for lower Southern Ocean surface nitrate concentrations during the last ice age. *Proc. Natl. Acad. Sci. U. S. A.* 114, 3352–3347. doi: 10.1073/pnas.1615718114

Wang, Y., and Cerling, T. E. (1994). A model of fossil tooth and bone diagenesis: Implications for paleodiet reconstruction from stable isotopes. *Palaeogeogr. Palaeoclimatol. Palaeoecol.* 107, 281–289. doi: 10.1016/0031-0182(94)90100-7

Weigand, M. A., Foriel, J., Barnett, B., Oleynik, S., and Sigman, D. M. (2016). Updates to instrumentation and protocols for isotopic analysis of nitrate by the denitrifier method. *Rapid Commun. Mass Spectrom.* 30, 1365–1383.

Wilson, D. E., and Mittermeier, R. A. (2009). *Handbook of the Mammals of the World*. Barcelona: Lynx Wsicions.

Wilson, E. O. (2014). *A window on eternity: A biologist's walk through Gorongosa National Park*. New York, NY: Simon and Schuster.

Wolf, J. (1960). “Der diurnale Säurerhythmus,” in *Plant Respiration Inclusive Fermentations and Acid Metabolism/Pflanzenatmung Einschliesslich Gärungen und Säurestoffwechsel. Encyclopedia of Plant Physiology / Handbuch der Pflanzenphysiologie*, ed. J. Wolf (Berlin: Springer), 1930–2010.

Yang, D., Uno, K. T., Souron, A., McGrath, K., Pubert, É., and Cerling, T. E. (2020). Intra-tooth stable isotope profiles in warthog canines and third molars: Implications for paleoenvironmental reconstructions. *Chem. Geol.* 554:119799. doi: 10.1016/j.chemgeo.2020.119799

Zazzo, A., Balasse, M., and Patterson, W. P. (2005). High-resolution $\delta^{13}\text{C}$ intratooth profiles in bovine enamel: Implications for mineralization pattern and isotopic attenuation. *Geochim. Cosmochim. Acta* 69, 3631–3642. doi: 10.1016/j.gca.2005.02.031

COPYRIGHT

© 2022 Lüdecke, Leichliter, Aldeias, Bamford, Biro, Braun, Capelli, Cybulski, Duprey, Ferreira da Silva, Foreman, Habermann, Haug, Martinez, Mathe, Mulch, Sigman, Vonhof, Bobe, Carvalho and Martinez-García. This is an open-access article distributed under the terms of the [Creative Commons Attribution License \(CC BY\)](https://creativecommons.org/licenses/by/4.0/). The use, distribution or reproduction in other forums is permitted, provided the original author(s) and the copyright owner(s) are credited and that the original publication in this journal is cited, in accordance with accepted academic practice. No use, distribution or reproduction is permitted which does not comply with these terms.